Time Adaptive Discrete Mechanics and Optimal Control

Keck Institute for Space Studies Graduate Student Fellowship Final Report
by
Ashley Moore

California Institute of Technology
Pasadena, California

2011

Acknowledgements

I would like to begin by thanking my advisor, Dr. Jerry Marsden. It was an honor and a pleasure to work under the guidance of such an inspiring, brilliant, and kind man.

A very special thanks is due to Dr. Sina Ober-Blöbaum, my closest collaborator and mentor for the past four years. Thanks for the Skype chats, for editing papers, for debugging code, and for teaching me just about everything I know about DMOC and how to do research. I can never really express my gratitude.

Thank you also to my committee members, Dr. Richard Murray, Dr. Mathieu Desbrun, and Dr. Michael Ortiz. In particular, thanks to Mathieu for many discussions on time adaption, and to Richard for serving as my advisor this year.

Furthermore, much appreciation is due to Dr. Sergio Pellegrino and my fellow KISS project memebers Marin Kobilarov, Gwen Johnson, Keith Patterson, Terry Gdoutos, Ayako Torisaka, Saturo Ozawa, Chiara Daraio, and Jim Breckenridge.

Finally, I wish to express my deepest gratitude to the Keck Institute for Space Studies for providing me with a KISS Graduate Student Fellowship this year. I am graduating on June 10, 2011, due in large part to this fellowship. The funding allowed me to focus exclusively on research. Particularly considering the tragic passing of my adivsor, Dr. Jerrold E. Marsden, the funding and project provided me with much needed continuity, mentorship, and support.

I have accepted a position at The Aerospace Corporation in El Segundo, CA and will begin work in the control analysis department in July. Aerospace supports a rather academic environment, and I hope to teach a course at a local university in my free time. I am very much looking forward to this next chapter in my career. Thanks again to the Keck Institute for the generous support and its pivotal role in my academic success.

Time Adaptive Discrete Mechanics and Optimal Control

by

Ashley Moore

Abstract

Space mission design is often achieved through a combination of dynamical systems theory and optimal control. This work focuses on how to adapt DMOC, a method devised with a constant step size, for the highly nonlinear dynamics involved in space problems including trajectory design and reconfiguration and docking of formation flying cubesats, similar to those proposed for the KISS project's reconfigurable modular space telescope. A time adaptive form of DMOC is developed that allows for a variable step size that is updated throughout the optimization process. Time adapted DMOC is based on a discretization of Hamilton's principle applied to the time adapted Lagrangian of the optimal control problem. Variations of the discrete action of the optimal control Lagrangian lead to discrete Euler-Lagrange equations that can be enforced as constraints for a boundary value problem. This new form of DMOC leads to the accurate and efficient solution of optimal control problems with highly nonlinear dynamics. Time adapted DMOC is tested on several space trajectory problems including the elliptical orbit transfer in the 2-body problem and the reconfiguration of a cubesat.

Contents

Chapter 1

Introduction

Space mission design is a complicated endeavor that often combines dynamical systems theory, optimization, and numerical techniques. For the KISS study on a reconfigurable modular space telescope, the reconfiguration and docking of the telescope's cubesat will be achieved using many different techniques, including optimization. Discrete mechanics and optimal control (DMOC) is a very useful tool that may be used to design the reconfiguration maneuver, ensuring that the cubesat approaches docking in the correct configuration with desirable velocity. DMOC is theoretically formulated for use with a constant step size, and even though it is possible to use DMOC with a variable step size, it is desirable to modify DMOC to allow the step size to evolve according to the dynamics.

This work focuses on the development of a time adaptive form of DMOC. First, a thorough derivation of variational integrators with time adaption is presented. Even though DMOC follows directly from the derivation of regular variational integrators, the same is not true with time adaption. Naively translating time adaptive variational integrators to time adaptive DMOC leads to incorrect optimization results, demonstrating that time adaption within the optimal control problem is more complicated. First, it is necessary to consider how to properly write the time adapted version of the optimal control Lagrangian. Then, discretization of Hamilton's principle applied to the optimal control Lagrangian leads to a different version of discrete Euler-Lagrange equations that serve as constraints for optimization. The proposed time adapted DMOC is now an indirect optimization method while regular DMOC is a direct method. The new method is tested on the elliptical orbit transfer problem and the reconfiguration of a formation flying cubesat.

Chapter 2

Background

This work combines and builds upon several topics within dynamical systems theory including variational integrators and optimal control, specifically, discrete mechanics and optimal control (DMOC). Therefore, an introduction to the theoretical background of each topic is warranted.

2.1 Variational Integrators

Variational Integrators are symplectic, momentum-preserving integrators derived from variational mechanics. The full development and analysis of discrete mechanics and variational integrators is presented in Marsden and West [9]. Before discussing the derivation of variational integrators, it is useful to begin with some definitions. Consider a mechanical system with configuration manifold Q, associated state space TQ and Lagrangian $L : TQ \to \mathbb{R}$. Following the conventions of [9], given a time interval $[0, T]$, the *path space* is defined by

$$\mathcal{C}(Q) = \mathcal{C}([0, T], Q) = \{q : [0, T] \to Q | q \text{ is a } C^2 \text{ curve}\}, \tag{2.1}$$

and the *action map* $\mathfrak{G} : \mathcal{C}(Q) \to \mathbb{R}$ is

$$\mathfrak{G}(q) \equiv \int_0^T L(q(t), \dot{q}(t))dt. \tag{2.2}$$

Hamilton's principle states that the evolution $q(t)$ of the system is a stationary point of the action. Therefore, variations of the action with fixed endpoints must be zero. For the Lagrangian system $L(q, \dot{q})$, this gives

$$\begin{aligned}
\delta \int_0^T L\left(q(t), \dot{q}(t)\right) dt &= \int_0^T \left[\frac{\partial L}{\partial q} \cdot \delta q + \frac{\partial L}{\partial \dot{q}} \cdot \delta \dot{q} \right] dt \\
&= \int_0^T \left[\frac{\partial L}{\partial q} - \frac{d}{dt}\left(\frac{\partial L}{\partial \dot{q}}\right)\right] \cdot \delta q \; dt + \left.\frac{\partial L}{\partial \dot{q}} \delta q \right|_0^T \\
&= \int_0^T \left[\frac{\partial L}{\partial q} - \frac{d}{dt}\left(\frac{\partial L}{\partial \dot{q}}\right)\right] \cdot \delta q \; dt = 0, \qquad (2.3)
\end{aligned}$$

where integration by parts is used to reformulate the $\delta\dot{q}$ term and the boundary term disappears because $\delta q(T) = \delta q(0) = 0$. For this expression to be zero for all δq, then the integrand must be zero, resulting in the continuous Euler-Lagrange equations

$$\frac{\partial L}{\partial q}(q, \dot{q}) - \frac{d}{dt}\left(\frac{\partial L}{\partial \dot{q}}(q, \dot{q})\right) = 0. \qquad (2.4)$$

The same derivation may be performed in the discrete framework using discrete variational mechanics. The state space TQ is replaced by $Q \times Q$ and the discretization grid is defined by $\Delta t = \{t_k = kh \,|\, k = 0, \ldots, N\}$, $Nh = T$, where N is a positive integer and h is the step size. The path $q : [0, T] \to Q$ is replaced by a discrete path $q_d : \{t_k\}_{k=0}^N \to Q$, where $q_k = q_d(kh)$ is an approximation to $q(kh)$[9, 11]. The continuous Lagrangian, $L(q, \dot{q})$, is replaced with a discrete Lagrangian, $L_d(q_k, q_{k+1}, h)$ using the midpoint rule

$$L_d(q_k, q_{k+1}, h) = hL\left(\frac{q_k + q_{k+1}}{2}, \frac{q_{k+1} - q_k}{h}\right), \qquad (2.5)$$

approximating the action integral along the curve between q_k and q_{k+1}. Thus it is possible to write

$$\int_0^T L(q, \dot{q}) \approx \sum_{k=0}^{N-1} L_d(q_k, q_{k+1}, h) \qquad (2.6)$$

where the integral has also been approximated using the midpoint rule. Note that it is possible to use more advanced quadrature rules to achieve integrators with a higher order of accuracy, but midpoint rule is exclusively used in this thesis.

Variations of the discrete action with respect to q_k gives

$$\begin{aligned}
\delta \sum_{k=0}^{N-1} & L_d(q_k, q_{k+1}, h) \\
&= \sum_{k=0}^{N-1} \left[D_1 L_d(q_k, q_{k+1}, h) \cdot \delta q_k + D_2 L_d(q_k, q_{k+1}, h) \cdot \delta q_{k+1}\right] \\
&= \sum_{k=0}^{N-1} \left[D_2 L_d(q_{k-1}, q_k, h) + D_1 L_d(q_k, q_{k+1}, h)\right] \cdot \delta q_k,
\end{aligned}$$

where discrete integration by parts and the condition that $\delta q_0 = \delta q_N = 0$ is used to arrive at the final expression. Note that D_1 (D_2) denotes the derivative with respect to the first (second) argument. The discrete Euler-Lagrange equations are obtained if the variations are required to vanish for all δq_k,

$$D_2 L_d(q_{k-1}, q_k, h) + D_1 L_d(q_k, q_{k+1}, h) = 0. \tag{2.7}$$

The discrete Legendre transform, also called discrete fibre derivatives, gives the discrete version of the standard Legendre transform, $p = \frac{\partial L}{\partial \dot{q}}$,

$$\mathbb{F}^+ L_d : (q_0, q_1) \mapsto (q_1, p_1) \quad = \quad (q_1, D_2 L_d(q_0, q_1)), \tag{2.8}$$

$$\mathbb{F}^- L_d : (q_0, q_1) \mapsto (q_0, p_0) \quad = \quad (q_0, -D_1 L_d(q_0, q_1)). \tag{2.9}$$

The left and right momenta may now be defined as

$$\begin{aligned}
p^+_{k,k+1} = p^+(q_k, q_{k+1}) = \mathbb{F}^+ L_d(q_k, q_{k+1}), \\
p^-_{k,k+1} = p^-(q_k, q_{k+1}) = \mathbb{F}^- L_d(q_k, q_{k+1}).
\end{aligned} \tag{2.10}$$

Recognizing that the Euler-Lagrange equations may be rewritten as

$$D_2 L_d(q_{k-1}, q_k) = -D_1 L_d(q_k, q_{k+1})$$

or

$$p^+_{k-1,k} = p^-_{k,k+1},$$

reveals that the Euler-Lagrange equations enforce momentum matching; that is, the momentum at a particular node k should be the same whether it is computed from above or below. Therefore, the momentum at each node k is given by

$$p_k = p^+_{k-1,k} = p^-_{k,k+1}. \tag{2.11}$$

In addition to preserving the momentum, variational integrators display excellent energy behavior. In particular, symplecticity guarantees no energy dissipation or growth for constant time steps [9].

2.1.1 Variational Integrators with Forcing

For a Lagrangian system with external forces $f(q(t), \dot{q}(t), u(t))$, where $u(t) \in U$ is a control parameter, the motion $q(t)$ must satisfy the Lagrange-d'Alembert principle,

$$\delta \int_0^T L(q(t), \dot{q}(t))\ dt + \int_0^T f(q(t), \dot{q}(t), u(t)) \cdot \delta q(t)\ dt = 0 \tag{2.12}$$

for all variations δq with $\delta q(0) = \delta q(T) = 0$. Integration by parts generates the forced Euler-Lagrange equations

$$\frac{d}{dt}\left(\frac{\partial L}{\partial \dot{q}}(q, \dot{q})\right) - \frac{\partial L}{\partial q}(q, \dot{q}) = f(q, \dot{q}, u). \tag{2.13}$$

The path q is discretized as before, and the control path $u : [0, T] \to U$ is replaced by a discrete one. To this end, a refined grid, $\Delta\tilde{t}$, is generated via a set of control points $0 \leq c_1 < \cdots < c_s \leq 1$ and $\Delta\tilde{t} = \{t_{k\ell} = t_k + c_\ell h \,|\, k = 0, \ldots, N-1; \ell = 1, \ldots, s\}$. With this notation, the discrete control path is defined to be $u_d : \Delta\tilde{t} \to U$. The intermediate control samples u_k on $[t_k, t_{k+1}]$ are defined as $u_k = (u_{k1}, \ldots, u_{ks}) \in U^s$ to be the values of the control parameters guiding the system from $q_k = q_d(t_k)$ to $q_{k+1} = q_d(t_{k+1})$, where $u_{kl} = u_d(t_{kl})$ for $l \in \{1, \ldots, s\}$. Then the continuous force $f(q, \dot{q}, u) : TQ \times U \to T^*Q$ is approximated by the discrete force $f_k(q_k, q_{k+1}, u_k)$ on the same time grid, $\Delta\tilde{t}$.

The continuous virtual work term in equation (2.12) is approximated by

$$f_k^- \cdot \delta q_k + f_k^+ \cdot \delta q_{k+1} \approx \int_{kh}^{(k+1)h} f(q(t), \dot{q}(t), u(t)) \cdot \delta q(t)\ dt, \tag{2.14}$$

where f_k^-, f_k^+ are the left and right discrete forces, respectively. The left and right discrete forces combine to represent the discrete force, f_k, such that

$$f_k(u_k)(q_k, q_{k+1}) \cdot (\delta q_k, \delta q_{k+1}) = f_k^+(u_k)(q_k, q_{k+1}) \cdot \delta q_{k+1} + f_k^-(u_k)(q_k, q_{k+1}) \cdot \delta q_k. \tag{2.15}$$

Note that f_{k-1}^+ may be viewed as the force acting on q_k during the time interval $[t_{k-1}, t_k]$, while f_k^- is the force on q_k applied during $[t_k, t_{k+1}]$. See [11] for more details. Therefore, the discrete Lagrange-d'Alembert principle requires the discrete curve $\{q_k\}_{k=0}^N$ to satisfy

$$\delta \sum_{k=0}^{N-1} L_d(q_k, q_{k+1}, h) + \sum_{k=0}^{N-1} \left[f_k^- \cdot \delta q_k + f_k^+ \cdot \delta q_{k+1} \right] = 0, \tag{2.16}$$

for all variations δq_k such that $\delta q_0 = \delta q_N = 0$. This is equivalent to the forced discrete Euler-Lagrange equations

$$D_2 L_d(q_{k-1}, q_k) + D_1 L_d(q_k, q_{k+1}) + f_{k-1}^+ + f_k^- = 0. \tag{2.17}$$

The forced discrete Legendre transform,

$$\begin{aligned} \mathbb{F}^{f+} L_d &: (q_{k-1}, q_k) \mapsto (q_k, p_k) = (q_k, D_2 L_d(q_{k-1}, q_k) + f_{k-1}^+) \\ \mathbb{F}^{f-} L_d &: (q_{k-1}, q_k) \mapsto (q_{k-1}, p_{k-1}) = (q_{k-1}, -D_1 L_d(q_{k-1}, q_k) - f_{k-1}^-), \end{aligned} \tag{2.18}$$

provides the definition for the discrete momentum,

$$p_k = D_2 L_d(q_{k-1}, q_k) + f_{k-1}^+ \tag{2.19}$$

$$p_{k-1} = -D_1 L_d(q_{k-1}, q_k) - f_{k-1}^-. \tag{2.20}$$

Even with external forces, variational integrators preserve the energy rate better than non-symplectic integrators. Specifically, the Forced Noether's theorem relates the momentum evolution and applied forces, guaranteeing that the Lagrangian momentum map is preserved. See [9] for more details.

2.1.2 Implementation

Given an initial condition (q_0, p_0), it is possible to compute q_1 from equation (2.20). Next, the discrete Euler-Lagrange equations provide a recursive rule for computing $\{q_{k+1}\}_{k=1}^{N-1}$ based on (q_{k-1}, q_k). The equations are most likely implicit and must be solved using an iterative solver such as Newton's method or Fsolve in MATLAB. With knowledge of the $\{q_k\}_{k=0}^{N}$, the momenta $\{p_k\}_{k=1}^{N}$ can be computed using equation (2.19).

2.1.3 Time Adaptive Variational Integrators

The variational integrators described above are valid for a constant step size, h. However, it is impractical to approach some systems using a constant step size. For example, the nonlinearity of the 3-body problem requires very small step size near bodies while coarser time stepping is sufficient elsewhere. Therefore, time adaption would be very useful in such a problem. However, if the step size is changed naively throughout the integration, the symplecticity can be destroyed. Therefore, care must be taken when including time adaption.

Hamiltonian Symplectic Integrators

Symplectic time adaptive integrators for Hamiltonian systems are proposed by Leimkuhler and Reich [8] and Hairer, Lubich, and Wanner [5] using a Sundman transformation,

$$\frac{dt}{d\tau} = \sigma(q, p), \tag{2.21}$$

where σ is a smooth function of position and momentum. Application of this transformation to a system with Hamiltonian $H(q, p)$ generates the equations of motion

$$\begin{aligned} q' &= \frac{dq}{d\tau} = \sigma(q,p)\nabla_p H(q,p) \\ p' &= \frac{dp}{d\tau} = -\sigma(q,p)\nabla_q H(q,p). \end{aligned} \tag{2.22}$$

In general, this system is no longer Hamiltonian. Therefore, the authors suggest a new Hamiltonian

$$\tilde{H}(q,p) = \sigma(q,p)(H(q,p) - H_0), \tag{2.23}$$

where H_0 is the energy and is constant along trajectories. The equations of motion for this system are given by

$$\begin{aligned} q' &= \sigma(q,p)\nabla_p H(q,p) + (H(q,p) - H_0)\nabla_p \sigma(q,p) \\ p' &= -\sigma(q,p)\nabla_q H(q,p) - (H(q,p) - H_0)\nabla_q \sigma(q,p). \end{aligned} \tag{2.24}$$

Since $H(q,p) - H_0 = 0$, this system reduces to the original system

$$\begin{aligned} q' &= \sigma(q,p)\nabla_p H(q,p) \to \dot{q} = \nabla_p H(q,p) \\ p' &= -\sigma(q,p)\nabla_q H(q,p) \to \dot{p} = -\nabla_q H(q,p). \end{aligned} \tag{2.25}$$

This idea will be very important for the derivation of DMOC with time adaption. Integration of the transformed system using fixed time steps in τ is equivalent to using variable time steps in t.

Note that, in general, a Hamiltonian and Lagrangian are related by the equations

$$\begin{aligned} H &= \frac{\partial L}{\partial \dot{q}} \cdot \dot{q} - L \\ L &= \frac{\partial H}{\partial p} \cdot p - H, \end{aligned} \tag{2.26}$$

if they are hyper-regular. Therefore, it is possible to write the time adapted

Lagrangian as

$$\begin{aligned}\tilde{L} &= \frac{\partial \tilde{H}}{\partial p}\cdot p - \tilde{H} = \frac{\partial \sigma(q,p)}{\partial p}(H - H_0)\cdot p + \sigma\left(\frac{\partial H}{\partial p}\cdot p - H + H_0\right) \\ &= \sigma(L + H_0).\end{aligned} \tag{2.27}$$

Time Adaption for Lagrangian Systems

In addition to a time-adaptive Hamiltonian formulation, it is desirable to develop the same ideas for a Lagrangian system. To this end, Kharevych [7] suggests adding a constraint to enforce the time step control directly into Hamilton's principle. Consider the time adaption rule

$$t_{k+1} - t_k = h\sigma(q_k, q_{k+1}), \tag{2.28}$$

where t_k are the discrete time points in t, $h = \tau_{k+1} - \tau_k$ is the constant time step in τ, and τ_k are the discrete time nodes in τ. The discrete, constrained action may be written

$$\widehat{S}_0^N = \sum_{k=0}^{N-1}\left[L_d(q_k, q_{k+1}, t_{k+1} - t_k) + \lambda_k(t_{k+1} - t_k - h\sigma(q_k, q_{k+1}))\right], \tag{2.29}$$

where λ_k is a Lagrange multiplier that enforces the time constraint. Variations with respect to q_k, t_k, and λ_k give

$$\begin{aligned}\delta\widehat{S}_0^N = &\left[D_1 L_{k,k+1} + D_2 L_{k-1,k} - h\lambda_{k-1}\frac{\partial\sigma(q_{k-1}, q_k)}{\partial q_k} - h\lambda_k\frac{\partial\sigma(q_k, q_{k+1})}{\partial q_k}\right]\cdot\delta q_k \\ &+ \Big[\lambda_{k-1} - \lambda_k + E_{k+1} - E_k\Big]\cdot\delta t_k + \Big[t_{k+1} - t_k - h\sigma(q_k, q_{k+1})\Big]\cdot\delta\lambda_k,\end{aligned} \tag{2.30}$$

where $L_{k,k+1} = L_d(q_k, q_{k+1}, t_{k+1} - t_k)$, $L_{k-1,k} = L_d(q_{k-1}, q_k, t_k - t_{k-1})$, and E_{k+1} is the discrete energy given by

$$E_{k+1} = -D_3 L_d(q_k, q_{k+1}, t_{k+1} - t_k). \tag{2.31}$$

Since the discrete Hamilton's principle requires that $\delta \widehat{S}_0^N = 0$, the time adapted discrete Euler Lagrange equations are given by

$$D_1 L_{k,k+1} + D_2 L_{k-1,k} - h\lambda_{k-1} \frac{\partial \sigma(q_{k-1}, q_k)}{\partial q_k} - h\lambda_k \frac{\partial \sigma(q_k, q_{k+1})}{\partial q_k} = 0, \tag{2.32a}$$

$$\lambda_k = \lambda_{k-1} + E_{k+1} - E_k, \tag{2.32b}$$

$$t_{k+1} = t_k + h\sigma(q_k, q_{k+1}). \tag{2.32c}$$

Kharevych [7] claims that these new time adapted discrete Euler-Lagrange equations are only a slight modification of the regular, fixed time step equations, and with λ_k sufficiently small, the integrator generates a discrete path with local flow near that of the original system while maintaining long time energy preservation. In particular, the discrete energy of the time adapted system,

$$\widehat{E}_{k+1} - \widehat{E}_1 = \lambda_k \sigma(q_k, q_{k+1}), \tag{2.33}$$

is preserved. This claim will be further explored in Chapter 3.

Lagrangian Systems with External and Dissipative Forces

A modification of the usual Lagrange-d'Alembert principle allows for the inclusion of external and dissipative forces in this time adaptive framework. The principle is now written

$$\delta \int_0^T L(q(t), \dot{q}(t))\ dt + \int_0^T f(q(t), \dot{q}(t), u(t))(\delta q - \dot{q}\delta t)\ dt = 0, \tag{2.34}$$

where the term $-\dot{q}\delta t$ is necessary because variations with respect to time are also considered. Using this variational principle, the forced, time adaptive discrete

Euler-Lagrange equations are

$$D_1 L_{k,k+1} + D_2 L_{k-1,k} - h\lambda_{k-1}\frac{\partial\sigma(q_{k-1}, q_k)}{\partial q_k} - h\lambda_k\frac{\partial\sigma(q_k, q_{k+1})}{\partial q_k} + f^+_{k-1} + f^-_k = 0, \tag{2.35a}$$

$$\lambda_k = \lambda_{k-1} + E_{k+1} - E_k - f^+_{k-1}\left(\frac{q_k - q_{k-1}}{h_{k-1}}\right) - f^-_k\left(\frac{q_{k+1} - q_k}{h_k}\right), \tag{2.35b}$$

$$t_{k+1} = t_k + h\sigma(q_k, q_{k+1}). \tag{2.35c}$$

where $f^+_k = f^-_k = \frac{h_k}{2} f_k$, $h_k = t_{k+1} - t_k$, and $h_{k-1} = t_k - t_{k-1}$. Integration of the regular time adapted system, equation (2.32), or the forced time adapted system, equation (2.35), requires q_0, q_1, t_0, t_1, and $\lambda_0 = 0$ to start. The implementation works as for a regular variational integrator with q_k, t_k, and λ_k computed simultaneously at each step.

2.2 Optimal Control

The basic ideas behind optimal control are necessary for an understanding of DMOC and particularly the development in Chapter 3. Ober-Blöbaum [11] provides a nice introduction and is summarized here. The goal of optimal control is to modify the dynamics of a system such that some quantity, for example the control effort, is minimized. More precisely, the objective functional is to be minimized subject to the system dynamics, initial conditions, and final constraints. Therefore, the optimal control problem, as used in this work, is defined as

$$\min_{x(\cdot), u(\cdot), (T)} J(x, u) = \int_0^T C(x(t), u(t))\, dt + \Phi(x(T)), \tag{2.36a}$$

$$\dot{x}(t) = f(x(t), u(t)), \tag{2.36b}$$

$$x(0) = x_0, \tag{2.36c}$$

$$0 = r(x(T)), \tag{2.36d}$$

where J is the objective functional, C is the cost function, $\Phi(x(T))$ is the Mayer term and is considered zero for this work, $\dot{x} = f(x(t), u(t))$ is the system of differential equations describing the dynamics, x_0 is a vector defining the initial condition, and $r(x(T))$ defines the final point constraint. Also note that the controls, $u(t)$, are constrained to the pointwise control constraint set $U = \{u(t) \in \mathbb{R}^{n_u} | h(u(t)) \geq 0\}$, and the final time T is held fixed.

The solution trajectory $\eta(t) = (x(\cdot), u(\cdot))$ is a feasible solution if the constraints, equations (2.36b)–(2.36d), are fulfilled. The solution trajectory $\eta(t) = (x^*, u^*)$ is an optimal solution of the optimal control problem if

$$J(x^*, u^*) \leq J(x, u) \tag{2.37}$$

for all feasible pairs (x, u). The solution $\eta(t) = (x^*, u^*)$ is a locally optimal solution if there exists a neighborhood $B_\delta(x^*, u^*), \delta > 0$ for which equation (2.37) is true for all feasible $(x, u) \in B_\delta(x^*, u^*)$. For such a solution, $x^*(t)$ is a locally optimal trajectory, and $u^*(t)$ is the locally optimal control.

Definition The *Hamiltonian* of the optimal control problem is given by the function $\mathcal{H} : \mathbb{R}^{n_x} \times \mathbb{R}^{n_u} \times \mathbb{R}^{n_x} \to \mathbb{R}$ and is defined by

$$\mathcal{H}(x, u, \lambda) = -C(x, u) + \lambda^T \cdot f(x, u), \tag{2.38}$$

where $\lambda_i, i = 1, \ldots, n_x$ are the adjoint variables, and n_x and n_u are the dimensions of the state, x, and control, u, respectively.

Definition The *Lagrangian* of the optimal control problem, equation (2.36), is a function $\mathcal{L} : \mathbb{R}^{n_x} \times \mathbb{R}^{n_u} \times \mathbb{R}^{n_x}$ given by

$$\mathcal{L}(\eta, \lambda) = C(x(t), u(t)) + \lambda^T(t) \cdot [\dot{x} - f(x(t), u(t))]. \tag{2.39}$$

The *action* of the optimal control Lagrangian is given by

$$\mathfrak{G}(\eta, \lambda) = \int_0^T \left(C(x(t), u(t)) + \lambda^T(t) \cdot [\dot{x} - f(x(t), u(t))] \right) dt. \tag{2.40}$$

The point $(\eta^*(t), \lambda^*(t))$ is a saddle point of the action if

$$(\eta(t), \lambda^*(t)) \leq \mathcal{L}(\eta^*(t), \lambda^*(t)) \leq \mathcal{L}(\eta^*(t), \lambda(t)) \ \forall \ (\eta(t), \lambda(t)). \tag{2.41}$$

Local solutions of the optimal control problem, equation (2.36), are saddle points of the action of the Lagrangian $\mathcal{L}$. Therefore, setting variations of the action of $\mathcal{L}$ with respect to η and λ to zero results in the Euler-Lagrange equations, which serve as necessary optimality conditions for the optimal control problem. This result is given by the Pontryagin Maximum Principle.

Theorem 2.2.1 (Pontryagin Maximum Principle) *Let (x^*, u^*) be an optimal solution of the optimal control problem, equation (2.36). Then, there exists a piecewise continuous differentiable function $\lambda : [0, T] \to \mathbb{R}^{n_x}$ and a vector $\alpha \in \mathbb{R}^{n_r}$ such that*

$$\mathcal{H}(x^*(t), u^*(t), \lambda(t)) = \max_{u(t) \in U} \mathcal{H}(x(t), u(t), \lambda(t)) \ \forall \ t \in [0, T], \tag{2.42a}$$

$$\dot{x}^*(t) = \nabla_\lambda \mathcal{H}(x^*(t), u^*(t), \lambda(t), \ x^*(0) = x_0, \tag{2.42b}$$

$$\dot{\lambda}(t) = -\nabla_x \mathcal{H}(x^*(t), u^*(t), \lambda(t)), \tag{2.42c}$$

$$\lambda(T) = \nabla_x(\Phi(x^*(T)) - \nabla_x r(x^*(T))\alpha. \tag{2.42d}$$

A proof of this theorem can be found in Pontryagin et al. [13]. Note that the proof is not based on the calculus of variations. Deriving the necessary optimality conditions via calculus of variations on the optimal control Lagrangian can be more intuitive and is valid only if the solution and controls are smooth enough.

There are many different approaches used for the numerical solution of optimal control problems. Most methods can be classified as either an indirect method or a direct method. Indirect methods are derived directly from the Pontryagin maximum principle and involve an explicit expression of the necessary conditions for optimality. For direct methods, the problem is transformed into a finite dimensional nonlinear programming problem. Some examples of indirect methods include *gradient methods*, *multiple shooting*, and *collocation*, while *direct shooting*, *direct multiple shooting*, and *direction collection* are examples of direct methods. Betts [1] and Binder et al. [2] provide good overviews of the algorithms used for different numerical optimization methods. DMOC (Discrete Mechanics and Optimal Control) can also be classified as a direct method.

2.2.1 DMOC

DMOC is an optimal control scheme closely related to variational integrators that was developed by Junge, Marsden, and Ober-Blöbaum [6, 11, 12]. It is based on a direct discretization of the Lagrange-d'Alembert principle of the mechanical system. The resulting forced discrete Euler-Lagrange equations are used as optimization constraints for a given cost function. The resulting restricted optimization problem is solved with an SQP solver.

Consider a mechanical system to be moved along a curve $q(t) \in Q$ during the time interval $t \in [0, T]$ from an initial state $(q^0, \dot{q}^0)$ to a final state $(q^T, \dot{q}^T)$ under the influence of a force $f(q(t), \dot{q}(t), u(t))$. The curves q and u are chosen to minimize a given objective functional,

$$J(q, \dot{q}, u) = \int_0^T C(q(t), \dot{q}(t), f(q(t), \dot{q}(t), u(t)))\, dt, \tag{2.43}$$

such that the system satisfies the Lagrange-d'Alembert principle,

$$\delta \int_0^T L(q(t), \dot{q}(t))\, dt + \int_0^T f(q(t), \dot{q}(t), u(t)) \cdot \delta q(t)\, dt = 0, \tag{2.44}$$

for all variations δq with $\delta q(0) = \delta q(T) = 0$.

The optimal control problem stated in equation (2.43) and equation (2.44) is transformed into a finite dimensional constrained optimization problem using a global discretization of the states and the controls, as described for variational integrators. Recall from §2.1, the discrete Lagrange-d'Alembert principle, equation (2.16), emerges using an approximation of the action integral in equation (2.44) by a discrete Lagrangian $L_d : Q \times Q \to \mathbb{R}$,

$$L_d(q_k, q_{k+1}) \approx \int_{kh}^{(k+1)h} L(q(t), \dot{q}(t))\ dt,$$

and discrete forces

$$f_k^- \cdot \delta q_k + f_k^+ \cdot \delta q_{k+1} \approx \int_{kh}^{(k+1)h} f(q(t), \dot{q}(t), u(t)) \cdot \delta q(t)\ dt, \tag{2.45}$$

where the left and right discrete forces $f_k^{\pm}$ now depend on (q_k, q_{k+1}, u_k). Then the discrete Lagrange-d'Alembert principle requires that,

$$\delta \sum_{k=0}^{N-1} L_d(q_k, q_{k+1}) + \sum_{k=0}^{N-1} \left(f_k^- \cdot \delta q_k + f_k^+ \cdot \delta q_{k+1} \right) = 0, \tag{2.46}$$

for all variations $\{\delta q_k\}_{k=0}^{N}$ with $\delta q_0 = \delta q_N = 0$.

The discrete cost function, C_d, approximates the continuous cost function, C, in a similar manner such that

$$C_d(q_k, q_{k+1}, f_k, f_{k+1}) \approx \int_{kh}^{(k+1)h} C(q, \dot{q}, f). \tag{2.47}$$

Therefore, the discrete objective functional is given by

$$J_d(q_d, f_d) = \sum_{k=0}^{N-1} C_d(q_k, q_{k+1}, f_k, f_{k+1}). \tag{2.48}$$

For the optimal control problem, it is also necessary to consider the boundary conditions. First, the discrete initial and final positions are required to match the continuous ones,

$$q_0 = q(0),$$
$$q_N = q(T).$$

The momentum boundary conditions require more care. The initial and final momentum of the continuous system is computed via the Legendre transform, $p = \frac{\partial L}{\partial \dot{q}}$,

$$p(0) = D_2 L(q_0, \dot{q}_0),$$
$$p(T) = D_2 L(q_N, \dot{q}_N).$$

Then requiring that $p(0) = p_0$ and $p(T) = p_N$, where p_0 and p_N are computed using the forced discrete Legendre transform, equations (2.19)–(2.20), generates the momentum boundary conditions,

$$\begin{aligned} D_2 L(q_0, \dot{q}_0) + D_1 L_d(q_0, q_1) + f_0^- &= 0, \\ -D_2 L(q_N, \dot{q}_N) + D_2 L_d(q_{N-1}, q_N) + f_{N-1}^+ &= 0. \end{aligned} \tag{2.49}$$

In summary, the discrete constrained optimization problem is given by

$$\min_{q_d, u_d} J_d(q_d, u_d) = \sum_{k=0}^{N-1} C_d(q_k, q_{k+1}, u_k), \tag{2.50a}$$

$$q_0 = q^0, \tag{2.50b}$$

$$q_N = q^T, \tag{2.50c}$$

$$D_2 L(q^0, \dot{q}^0) + D_1 L_d(q_0, q_1) + f_0^- = 0, \tag{2.50d}$$

$$D_2 L_d(q_{k-1}, q_k) + D_1 L_d(q_k, q_{k+1}) + f_{k-1}^+ + f_k^- = 0, \tag{2.50e}$$

$$-D_2 L(q^T, \dot{q}^T) + D_2 L_d(q_{N-1}, q_N) + f_{N-1}^+ = 0, \tag{2.50f}$$

with $k = 1, ..., N-1$.

Balancing accuracy and efficiency, the discrete cost function, C_d, the discrete Lagrangian, L_d, and the discrete forces are approximated with the midpoint rule, and constant control parameters are assumed on each time interval with $l = 1$ and $c_1 = \frac{1}{2}$,

$$C_d(q_k, q_{k+1}, u_k) = hC\left(\frac{q_{k+1} + q_k}{2}, \frac{q_{k+1} - q_k}{h}, u_k\right), \tag{2.51}$$

$$L_d(q_k, q_{k+1}) = hL\left(\frac{q_{k+1}+q_k}{2}, \frac{q_{k+1}-q_k}{h}\right), \tag{2.52}$$

$$f_k^- = f_k^+ = \frac{h}{2} f\left(\frac{q_{k+1}+q_k}{2}, \frac{q_{k+1}-q_k}{h}, u_k\right). \tag{2.53}$$

The order of approximation of the discrete Lagrangian, equation (2.52), and the discrete forces, equation (2.53), determines the order of convergence of the optimal control scheme. Therefore, second-order convergence is expected with this form of DMOC.

Equation (2.50) describes a nonlinear optimization problem with equality constraints, which can be solved by standard optimization methods like SQP, such as SNOPT [4]. Optionally, inequality constraints on states and controls can be included. In contrast to other direct optimal control methods, DMOC is based on the discretization of the variational principle, equation (2.44), rather than a discretization of the ordinary differential equations. In Ober-Blöbaum, Junge, and Marsden [12], a detailed analysis of DMOC resulting from this discrete variational approach is given. The optimization scheme is symplectic-momentum consistent, i.e., the symplectic structure and the momentum maps corresponding to symmetry groups are consistent with the control forces for the discrete solution independent of the step size h. Thus, the use of DMOC leads to a reasonable approximation to the continuous solution, also for large step sizes, i.e., a small number of discretization points. Also, the discrete solution inherits structural properties from the continuous system, e.g., good energy preservation or correct energy drift in the presence of external forces [9].

Chapter 3

Time Adaptive DMOC

3.1 Introduction

It is impractical to optimize nonlinear problems, particularly those in space mission design, using DMOC with a constant step size. Different strategies can be employed to circumvent this issue such as using sections of constant step size or using mesh refinement to design the step size profile, as described in [10]. However, it is desirable to develop a form of DMOC that allows for variable step size while maintaining the convergence and energy properties expected for DMOC. Furthermore, full time adaption should allow for the step size, determined by the dynamics, to be updated during the optimization. Time adaptive DMOC builds on the time adaption strategy developed for variational integrators described by Kharevych in [7]. However, the transition from time adaptive variational integrators to time adaptive DMOC is not as obvious as it may initially seem.

This chapter begins by describing Lagrangian mechanics with time adaption, setting the stage for a clear derivation and analysis of time adaptive variational integrators. The most obvious, and incorrect, attempt at translating time adaptive variational integrators to DMOC is presented to demonstrate why time adaptive DMOC requires different considerations than variational integrators. Next, a correct method for approaching time adaption for the optimal control problem is described. The method is validated with a simple example before proceeding with more interesting examples, including the elliptical orbit transfer problem and the reconfiguration of a cubesat.

3.2 Lagrangian Mechanics with Time Adaption

Before the derivation of time adaptive DMOC is presented, it is necessary to fully understand the derivation of variational integrators with time adaption. First consider a continuous system with configuration variables and time as functions of the parameter τ. This idea originates with the development of variational integrators for collision by Fetecau, Marsden, Ortiz, and West [3].

Following their notation, it is necessary to present some of their definitions. Consider a configuration manifold Q, and let the path space be defined as

$$\mathcal{M} = \mathcal{T} \times \mathcal{Q}([0, \tau_F], Q),$$

where

$$\mathcal{T} = \{c_t \in C^\infty([0, \tau_F], \mathbb{R}) | c_t' > 0 \text{ in } [0, \tau_F]\},$$
$$\mathcal{Q}([0, \tau_F], Q) = \{c_q : [0, \tau_F] \to Q | c_q \text{ is a } C^2 \text{ curve}\}.$$

A path $c \in \mathcal{M}$ is a pair $c = (c_t, c_q)$. Thus, given a path defined in this way, the associated path $q : [c_t(0), c_t(\tau_F)] \to Q$ is given by

$$q(t) = c_q({c_t}^{-1}(t)). \tag{3.1}$$

Equivalently, $c_q(\tau) = q(t)$, where τ is a time parameter. It is useful to note that c_q' denotes derivatives of c_q with respect to τ and $\dot{q}$ denotes derivatives of q with respect to t. With this in mind,

$$c_q' = \frac{dq}{d\tau}, \tag{3.2}$$

$$c_t' = \frac{dt}{d\tau}, \tag{3.3}$$

$$\dot{q} = \frac{c_q'}{c_t'}. \tag{3.4}$$

The action map $\mathfrak{G} : \mathcal{M} \to \mathbb{R}$ for the Lagrangian system in this new setting is given by

$$\mathfrak{G}(c_t, c_q) = \int_0^{\tau_f} L\left(c_q(\tau), \frac{c_q'(\tau)}{c_t'(\tau)}\right) c_t'(\tau) d\tau. \tag{3.5}$$

The action map for the associated curve q may be written

$$\mathfrak{G}(q) = \int_{c_t(0)}^{c_t(\tau_f)} L(q(s), \dot{q}(s)) ds, \tag{3.6}$$

where $s = c_t(\tau)$ is the change of coordinates.

3.2.1 Continuous System with Time Adaption

Now, consider a Lagrangian system with time adaption. From §2.1.3, a time adapted Lagrangian is given by

$$\tilde{L}(q(t), \dot{q}(t)) = \sigma(q) \left(L(q(t), \dot{q}(t)) + H_0\right), \tag{3.7}$$

where the time adaption will be enforced such that

$$c_t' = \frac{dt}{d\tau} = \sigma(q). \tag{3.8}$$

$\tilde{L}$ may be transformed into τ coordinates by

$$\tilde{L}\left(c_q(\tau), \frac{c_q'(\tau)}{c_t'(\tau)}\right) = \sigma(c_q(\tau)) \left(L\left(c_q(\tau), \frac{c_q'(\tau)}{c_t'(\tau)}\right) + H_0\right). \tag{3.9}$$

For ease of notation, (τ) will not be included henceforth, but it is implied. Equation (3.9) may equivalently be written

$$\tilde{L}\left(c_q, \frac{c_q'}{c_t'}\right) = \left(L\left(c_q, \frac{c_q'}{c_t'}\right) + H_0\right) \cdot c_t' + c_\lambda \cdot (c_t' - \sigma(c_q)), \tag{3.10}$$

where $c_\lambda(\tau) = \lambda(t)$ is a Lagrange multiplier that enforces the time adaption constraint, $c_t' = \sigma(c_q)$. Therefore, the action map of the time adapted system is given by

$$\mathfrak{G}(c_t, c_q, c_\lambda) = \int_0^{\tau_f} \left(L\left(c_q(\tau), \frac{c_q'(\tau)}{c_t'(\tau)}\right) + H_0\right) \cdot c_t' + c_\lambda \cdot (c_t' - \sigma(c_q))\; d\tau, \tag{3.11}$$

where the path c is now represented by $c = (c_t, c_q, c_\lambda)$. Variations of the action map with respect to the path gives

$$\begin{aligned} \delta \int_0^{\tau_f} \left(L\left(c_q(\tau), \frac{c_q'(\tau)}{c_t'(\tau)}\right) + H_0\right) \cdot c_t' + c_\lambda \cdot (c_t' - \sigma(c_q))\; d\tau = \\ \int_0^{\tau_f} \left(\left[\frac{\partial L}{\partial q} \cdot \delta c_q + \frac{\partial L}{\partial \dot{q}} \left(\frac{\delta c_q'}{c_t'} - \frac{c_q' \delta c_t'}{(c_t')^2}\right)\right] c_t' + c_\lambda \left(\delta c_t' - \frac{\partial \sigma}{\partial q} \cdot \delta c_q\right) \right. \\ \left. + (L + H_0)\delta c_t' + (c_t' - \sigma(c_q))\delta c_\lambda \right) d\tau. \end{aligned}$$

Multiple applications of integration by parts and the requirement that variations vanish on the endpoints generates the equations of motion,

$$\frac{d}{d\tau}\frac{\partial L}{\partial \dot{q}} - \frac{\partial L}{\partial q} c_t' + c_\lambda \frac{\partial \sigma}{\partial q} = 0 \tag{3.12}$$

$$\frac{d}{d\tau}\left(\frac{\partial L}{\partial \dot{q}}\frac{{c_q}'}{{c_t}'} - L - H_0 - c_\lambda\right) = 0 \tag{3.13}$$

$${c_t}' - \sigma(c_q) = 0. \tag{3.14}$$

Incorporating equation (3.14) into equation (3.12), recognizing that $\frac{\partial L}{\partial \dot{q}} \frac{c_q'}{c_t'} - L = E$ and $H_0 = E_0$, the initial energy, and transforming to t coordinates gives

$$\frac{d}{dt}\frac{\partial L}{\partial \dot{q}} - \frac{\partial L}{\partial q} + \frac{\lambda}{\sigma}\frac{\partial \sigma}{\partial q} = 0, \tag{3.15a}$$

$$\frac{d}{dt}(E - E_0 - \lambda) = 0. \tag{3.15b}$$

3.2.2 Continuous System with Time Adaption and Forces

The force term for the associated curve q,

$$\int_0^T f\left(q(t), \dot{q}(t), u(t)\right) \delta q(t)\ dt, \tag{3.16}$$

may be rewritten considering the transformation $\delta q(t) = \delta c_q - \frac{c_q'}{c_t'} \delta c_t$,

$$\begin{aligned} &\int_0^T f\left(q(t), \dot{q}(t), u(t)\right) \delta q(t)\ dt = \\ &\qquad \int_0^{\tau_f} \left(f\left(c_q, \frac{c_q'}{c_t'}, c_u\right) c_t' \cdot \delta c_q - f\left(c_q, \frac{c_q'}{c_t'}, c_u\right) c_q' \cdot \delta c_t \right) d\tau, \end{aligned} \tag{3.17}$$

where $dt = c_t'\ d\tau$, and c_u is the control parameter in τ coordinates. The Lagrange-d'Alembert principle requires that

$$\begin{aligned} &\delta \int_0^{\tau_f} \left(L\left(c_q, \frac{c_q'}{c_t'}\right) + H_0 \right) \cdot c_t' + c_\lambda \cdot (c_t' - \sigma(c_q)) d\tau + \\ &\qquad \int_0^{\tau_f} \left(f\left(c_q, \frac{c_q'}{c_t'}, c_u\right) c_t' \cdot \delta c_q - f\left(c_q, \frac{c_q'}{c_t'}, c_u\right) c_q' \cdot \delta c_t \right) d\tau = 0, \end{aligned} \tag{3.18}$$

for all variations δc_q, δc_t, and δc_λ, with $\delta c_q(0) = \delta c_q(\tau_f) = 0$, and $\delta c_t(0) = \delta c_t(\tau_f) = 0$, and $\delta c_\lambda(0) = \delta c_\lambda(\tau_f) = 0$. This principle gives the forced equations of motion, written in t coordinates, with H_0 replaced by E_0,

$$\frac{d}{dt}\frac{\partial L}{\partial \dot{q}} - \frac{\partial L}{\partial q} + \frac{\lambda}{\sigma}\frac{\partial \sigma}{\partial q} = f, \tag{3.19a}$$

$$\frac{d}{dt}(E - E_0 - \lambda) = f\dot{q}. \tag{3.19b}$$

3.2.3 Correspondence Between Original System and Time Adapted System

If $(q, \dot{q})$ is a solution of the regular Euler-Lagrange equations,

$$\frac{d}{dt}\frac{\partial L}{\partial \dot{q}} - \frac{\partial L}{\partial q} = 0, \tag{3.20a}$$
$$\frac{dE}{dt} = 0, \tag{3.20b}$$

then $(q, \dot{q}, \lambda)$ is a solution of the time adapted Euler-Lagrange equations,

$$\frac{d}{dt}\frac{\partial L}{\partial \dot{q}} - \frac{\partial L}{\partial q} + \frac{\lambda}{\sigma}\frac{\partial \sigma}{\partial q} = 0, \tag{3.21a}$$
$$\frac{d}{dt}\left(E - E_0 - \lambda\right) = 0, \tag{3.21b}$$

if $\lambda = 0$.

Proof Plug equation (3.20a) and $\lambda = 0$ into the right-hand side of equation (3.21a), verifying that $(q, \dot{q}, \lambda = 0)$ is a solution of equation (3.21a). Equation (3.21b) also holds because $\frac{d}{dt}E_0 = 0$ since E_0 is a constant, $\frac{d}{dt}\lambda = 0$ by definition of λ, and $\frac{d}{dt}E = 0$ according to equation (3.20b). $\square$

Conversely, if $(q, \dot{q}, \lambda)$ is a solution of the time adapted Euler-Lagrange equations, equations (3.21), restricted to the energy surface $E = E_0$, then $(q, \dot{q})$ is also a solution of the regular Euler-Lagrange equations if $\lambda(0) = 0$.

Proof Equation (3.21b) gives that $\frac{d}{dt}(E - E_0) = \frac{d}{dt}\lambda$. Since $E = E_0$, then $\frac{d}{dt}\lambda = 0$, and $\lambda = 0$ because $\lambda(0) = 0$. With $\lambda = 0$, equations (3.21) are equivalent to equations (3.21b). $\square$

Numerically, λ converges to zero with second-order convergence; thus the time adapted system converges to the original system in the limit as the step size converges to zero. Note that λ also converges to zero when the system includes forces.

3.2.4 Discrete System with Time Adaption

Before defining the discrete version of relevant integrals, it is necessary to define the discrete step sizes for both t and τ,

$$d\tau = \tau_{k+1} - \tau_k = h, \tag{3.22}$$

$$dt = t_{k+1} - t_k = h_k. \tag{3.23}$$

The action integral may be approximated according to the following quadrature rules,

$$\int_0^{\tau_f} L\left(c_q, \frac{{c_q}'}{{c_t}'}\right) \cdot {c_t}'(\tau)\ d\tau \approx \sum_{k=0}^{N-1} \bar{L}_d(q_k, q_{k+1}, h, h_k)\frac{h_k}{h}, \tag{3.24}$$

$$\int_0^{T} L(q(t), \dot{q}(t))\ dt \approx \sum_{k=0}^{N-1} L_d(q_k, q_{k+1}, h_k), \tag{3.25}$$

where

$$\bar{L}_d = hL\left(\frac{q_k + q_{k+1}}{2}, \frac{q_{k+1} - q_k}{h_k}\right), \tag{3.26}$$

$$L_d = h_k L\left(\frac{q_k + q_{k+1}}{2}, \frac{q_{k+1} - q_k}{h_k}\right). \tag{3.27}$$

Based on the definitions of $\bar{L}_d$ and L_d, the right-hand sides of equation (3.24) and equation (3.25) are equivalent.

Similarly,

$$\begin{aligned}\int_0^{\tau_f} c_{\lambda_k}({c_t}' - \sigma(c_q))d\tau &\approx \sum_{k=0}^{N-1} h\lambda_k\left(\frac{h_k}{h} - \sigma(q_k, q_{k+1})\right) \\ &= \sum_{k=0}^{N-1} \lambda_k\left(h_k - h\sigma(q_k, q_{k+1})\right),\end{aligned} \tag{3.28}$$

and

$$\int_{kh}^{(k+1)h} f\left(c_q, \frac{c_q{}'}{c_t{}'}, c_u\right) c_t{}' \delta c_q \; d\tau \approx \sum_{k=0}^{N-1} \left[f_k^-(q_k, q_{k+1}, u_k)\delta q_k + f_k^+(q_k, q_{k+1}, u_k)\delta q_{k+1}\right]$$
$$= \sum_{k=0}^{N-1} \left[f_k^-(q_k, q_{k+1}, u_k)\delta q_k + f_k^+(q_k, q_{k+1}, u_k)\delta q_{k+1}\right], \tag{3.29}$$

where $f_k^- = f_k^+ = \frac{h_k}{2} f_k$. The next part of the force integral may be approximated by

$$\int_{kh}^{(k+1)h} f\left(c_q, \frac{c_q{}'}{c_t{}'}, c_u\right) c_q' \delta c_t \; d\tau \approx$$
$$\sum_{k=0}^{N-1} \left[f_k^-(q_k, q_{k+1}, u_k)\frac{q_{k+1} - q_k}{h_k}\delta t_k + f_k^+(q_k, q_{k+1}, u_k)\frac{q_{k+1} - q_k}{h_k}\delta t_{k+1}\right]$$
$$= \sum_{k=0}^{N-1} \frac{h_k}{h} \left[f_k^-(q_k, q_{k+1}, u_k)\left(\frac{q_{k+1} - q_k}{h_k}\right)\delta t_k + f_k^+(q_k, q_{k+1}, u_k)\left(\frac{q_{k+1} - q_k}{h_k}\right)\delta t_{k+1}\right]. \tag{3.30}$$

Based on these approximations, the discrete action principle may be written

$$\delta \sum_{k=0}^{N-1} \left[L_d(q_k, q_{k+1}, h_k) + h_k H_0 + \lambda_k (h_k - h\sigma(q_k, q_{k+1}))\right]$$
$$+ \sum_{k=0}^{N-1} \left[f_k^-(q_k, q_{k+1}, u_k) \cdot (\delta q_k - \frac{q_{k+1} - q_k}{h_k}\delta t_k)\right]$$
$$+ \sum_{k=0}^{N-1} \left[f_k^+(q_k, q_{k+1}, u_k) \cdot (\delta q_{k+1} - \frac{q_{k+1} - q_k}{h_k}\delta t_{k+1})\right] = 0. \tag{3.31}$$

Variations with respect to q_k, λ_k, and t_k generate the discrete Euler-Lagrange equations as well as equations enforcing the time adaption and energy dissipation,

$$
\begin{aligned}
&D_1 L_d(q_k, q_{k+1}, h_k) + D_2 L_d(q_{k-1}, q_k, h_{k-1}) \\
&\qquad - h\lambda_k \frac{\partial \sigma(q_k, q_{k+1})}{\partial q_k} - h\lambda_{k-1} \frac{\partial \sigma(q_{k-1}, q_k)}{\partial q_k} + f_k^- + f_{k-1}^+ = 0, && \text{(3.32a)} \\
&t_{k+1} = t_k + h\sigma(q_k, q_{k+1}), && \text{(3.32b)} \\
&\lambda_k = \lambda_{k-1} + E_{k+1} - E_k - f_k^- \left(\frac{q_{k+1} - q_k}{h_k} \right) - f_{k-1}^+ \left(\frac{q_k - q_{k-1}}{h_{k-1}} \right), && \text{(3.32c)}
\end{aligned}
$$

where

$$
E_{k+1} = -D_3 L_d(q_k, q_{k+1}, t_{k+1} - t_k). \tag{3.33}
$$

Equations (3.32) are exactly the variational integrator equations with time adaption presented by [7]. However, note that the notation used here differs slightly from the notation used in [7], particularly for the external forces.

Preservation Properties

Since the usual Euler-Lagrange equations include energy preservation, it is useful to analyze the time adapted system to determine what quantities, if any, are conserved. Consider the system of equations for the time adapted continuos system given by equation (3.15). Manipulation of equation (3.15b) gives

$$
\begin{aligned}
\frac{d}{dt}\lambda &= \frac{d}{dt}E && \text{(3.34a)} \\
\dot{\lambda} &= \frac{d}{dt}\left(\frac{\partial L}{\partial \dot{q}} \dot{q} - L \right) && \text{(3.34b)} \\
\dot{\lambda} &= \left(\frac{d}{dt}\left(\frac{\partial L}{\partial \dot{q}} \right) - \frac{\partial L}{\partial q} \right) \dot{q}. && \text{(3.34c)}
\end{aligned}
$$

Using the relation from equation (3.15a),

$$\dot{\lambda} + \frac{\lambda}{\sigma}\frac{\partial \sigma}{\partial q}\dot{q} = 0 \tag{3.35a}$$

$$\dot{\lambda}\sigma + \lambda\frac{\partial \sigma}{\partial q}\dot{q} = 0 \tag{3.35b}$$

$$\frac{d}{dt}(\lambda \cdot \sigma) = 0. \tag{3.35c}$$

Hence, $\lambda \cdot \sigma$ is a conserved quantity. Since $\dot{\lambda} = \dot{E}$, it follows that

$$\lambda(t) = \lambda_0 + E(t) - E(0) = E(t) - E(0), \tag{3.36}$$

because $\lambda_0 = 0$ by definition. Therefore, the time adapted energy being preserved is

$$\hat{E}(t) = \lambda(t)\sigma = (E(t) - E(0)) \cdot \sigma(q). \tag{3.37}$$

Rearranging this equation, it is clear that

$$E(t) - E(0) = \frac{\hat{E}(t)}{\sigma(q)}, \tag{3.38}$$

and if σ is bounded from below, it gives a bound on the energy drift [7].

The new time adapted continuous system may be written

$$\frac{d}{dt}\frac{\partial L}{\partial \dot{q}} - \frac{\partial L}{\partial q} + \frac{\lambda}{\sigma}\frac{\partial \sigma}{\partial q} = 0, \tag{3.39}$$

$$\frac{d}{dt}(\lambda \cdot \sigma) = \frac{d}{dt}\left(\hat{E}\right) = 0, \tag{3.40}$$

where $\hat{E}$ is the quantity being preserved.

Analyzing the system from a discrete perspective, consider variations of the discrete action

$$\delta \sum_{k=0}^{N-1} \left[L_d(q_k, q_{k+1}, h_k) + h_k H_0 + \lambda_k(h_k - (\tau_{k+1} - \tau_k)\sigma(q_k, q_{k+1}))\right] = 0, \tag{3.41}$$

with respect to τ_k for a modified mechanical system with constant step size $h =$

$\tau_{k+1} - \tau_k$. This generates the difference in discrete energy,

$$\widehat{E}_{k+1} - \widehat{E}_k = \lambda_k \sigma(q_k, q_{k+1}) - \lambda_{k-1}\sigma(q_{k-1}, q_k), \tag{3.42}$$

for the modified system. Applying recursion relationships and $\lambda_0 = 0$, this may be written as

$$\widehat{E}_{k+1} - \widehat{E}_1 = \lambda_k \sigma(q_k, q_{k+1}) = (E_{k+1} - E_1)\sigma(q_k, q_{k+1}). \tag{3.43}$$

Since $\widehat{E}_{k+1} - \widehat{E}_1$ defines the energy drift for a variational integrator with constant step size, h, the modified discrete system inherits the usual energy preservation properties. Specifically, the energy drift is bounded such that $|\widehat{E}_{k+1} - \widehat{E}_1| = \mathcal{O}(h^2)$. This relationship can be used to bound the energy of the time adapted system. In particular,

$$|E_{k+1} - E_1| = \left| \frac{\widehat{E}_{k+1} - \widehat{E}_1}{\sigma(q_k, q_{k+1})} \right| = \mathcal{O}\left(\frac{h^2}{\sigma_{min}} \right), \tag{3.44}$$

because σ is bounded from below by σ_{min}. Therefore, even though the discrete energy may drift further from the initial value than for integration with constant time steps, the drift is still bounded with no error accumulation.

Preservation Properties with Forces

For a system with forces, it is important to see how the forces affect the energy evolution. The analysis proceeds as before, beginning by rewriting equation (3.19b) as

$$\begin{gathered} \frac{d}{dt}E - \frac{d}{dt}\lambda = f\dot{q} \\ \frac{d}{dt}\left(\frac{\partial L}{\partial \dot{q}}\right)\dot{q} - \frac{\partial L}{\partial q}\dot{q} - \frac{d}{dt}\lambda = f\dot{q}. \end{gathered} \tag{3.45}$$

Replace f with the left-hand side of equation (3.19a),

$$\begin{aligned}
\frac{d}{dt}\left(\frac{\partial L}{\partial \dot{q}}\right)\dot{q} - \frac{\partial L}{\partial q}\dot{q} - \frac{d}{dt}\lambda &= -\left(\frac{\partial L}{\partial q} - \frac{d}{dt}\frac{\partial L}{\partial \dot{q}} - \frac{\lambda}{\sigma}\frac{\partial \sigma}{\partial q}\right)\dot{q} \\
\frac{d}{dt}\left(\frac{\partial L}{\partial \dot{q}}\right)\dot{q} - \frac{\partial L}{\partial q}\dot{q} - \frac{d}{dt}\lambda &= \left(\frac{d}{dt}\frac{\partial L}{\partial \dot{q}} - \frac{\partial L}{\partial q} + \frac{\lambda}{\sigma}\frac{\partial \sigma}{\partial q}\right)\dot{q} \qquad (3.46) \\
\frac{d}{dt}\lambda\sigma + \lambda\frac{\partial \sigma}{\partial q}\dot{q} &= 0 \\
\frac{d}{dt}(\lambda\cdot\sigma) &= 0, \qquad (3.47)
\end{aligned}$$

so $\lambda \cdot \sigma$ is a conserved quantity, as before. From equation (3.19b),

$$\dot{\lambda} = \frac{dE}{dt} - f\dot{q}, \qquad (3.48)$$

$$\lambda(t) = E(t) - E(0) - \int_0^t f(q(s), \dot{q}(s), u(s))\dot{q(s)}\ ds. \qquad (3.49)$$

Tthe time adapted energy being preserved is

$$\hat{E} = \lambda\cdot\sigma = \left(E(t) - E(0) - \int_0^t f(q(s), \dot{q}(s), u(s))\dot{q}(s)\ ds\right)\sigma. \qquad (3.50)$$

Rearranging this equation,

$$\frac{\hat{E}(t)}{\sigma(q)} = E(t) - E(0) - \int_0^t f(q(s), \dot{q}(s), u(s))\dot{q}(s)\ ds. \qquad (3.51)$$

The energy should evolve according to the integral of the applied forces, and since $\hat{E}(t)$ is preserved and σ is bounded from below, there is a bound on the drift in true energy evolution.

Considering the discrete formulation, the energy drift is bounded by

$$|E_{k+1} - E_1 - \sum_{i=1}^{k} f_{i-1}^{+}(q_j - q_{j-1}) + f_i^{-}(q_{j+1} - q_j)| = \mathcal{O}\left(\frac{h^2}{\sigma_{min}}\right). \qquad (3.52)$$

3.3 Naive Time Adaption for DMOC

Since the regular form of DMOC is directly related to variational integrators, it appears that the time adapted form of DMOC should also be related to time adapted variational integrators. However, this assumption is incorrect as demonstrated with a simple optimal control example. Consider the simple system with Lagrangian, $L = \frac{1}{2}\dot{q}^2$. The controlled equations of motion are

$$\ddot{q} = u, \tag{3.53}$$

where u is the control force. The goal is to move the system from some initial condition $(q_0, \dot{q}_0)$ to the final condition $(q_N, \dot{q}_N)$ while minimizing the control effort; therefore, the cost function is $C = \frac{1}{2}u^2$. The analytical solution to this optimal control problem is given by

$$q(t) = c_1 + c_2 t + \frac{c_3}{2}t^2 + \frac{c_4}{6}t^3, \tag{3.54a}$$

$$u(t) = c_4 t + c_3, \tag{3.54b}$$

where the constants c_1, c_2, c_3, and c_4 are determined by the boundary conditions,

$$\begin{aligned}
c_1 &= q_0, \\
c_2 &= \dot{q}_0, \\
c_3 &= -\frac{2}{t_N^2}\left((2\dot{q}_0 + \dot{q}_N)t_N + 3(q_0 - q_N)\right), \\
c_4 &= \frac{6}{t_N^3}\left((\dot{q}_0 + \dot{q}_N)t_N + 2(q_0 - q_N)\right).
\end{aligned}$$

Now consider a specific example on the time interval $[0, 10]$ with boundary conditions $q_0 = 1$, $\dot{q}_0 = 1$, $q_N = 11$, and $\dot{q}_N = 0$. A time adapted initial guess is created using equation (3.32) with $f = u = 0$ and $\sigma = \frac{q}{2}$. This initial guess is optimized using the time adapted equations, equations (3.32), as optimization constraints and with control force $f = u$ an optimization variable. As before, the discrete objective function is given by

$$J_d = \sum_{k=0}^{N-1} \frac{h}{2} u_k^2.$$

Successful optimization generates the trajectory and control profile shown in Figure 3.1. The analytical solutions for the trajectory $q(t)$ and control $u(t)$, based on equation (3.54) are included. It is obvious from the optimized control profile shown in Figure 3.1(b), that the optimizer converges to a different optimal solution. Even if the true solution is used as the initial guess, the incorrect solution is still generated. This result indicates that the equations that work for time adapted variational integrators do not directly translate to a time adapted form of DMOC. The effect of time adaption on control forces and the optimal control problem must be considered.

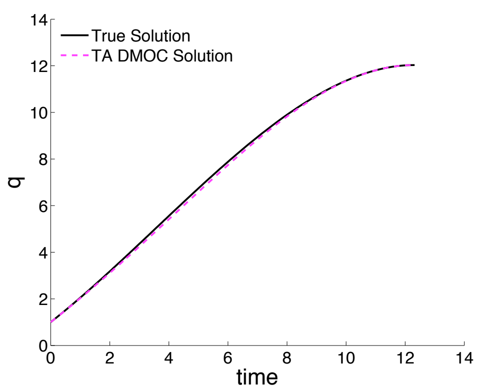

(a) Optimal Trajectory, $q(t)$

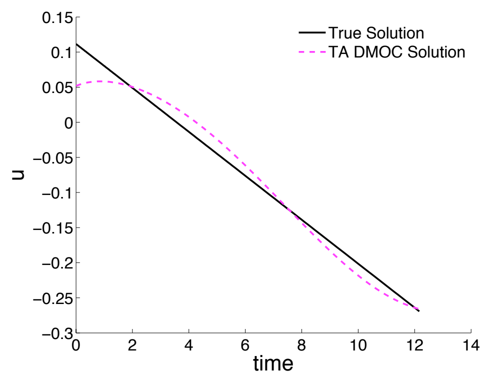

(b) Optimal Control, $u(t)$

Figure 3.1: Naive formulation of time adapted DMOC leads to incorrect optimal solution both for the (a) optimal trajectory and (b) optimal control force.

3.4 Time Adaption for Optimal Control Problem

To understand how to properly employ time adaption with DMOC, it is necessary to begin by determining how the optimal control Lagrangian $\mathcal{L}$ is computed using the optimal control Hamiltonian $\mathcal{H}$. Then, this relationship may be exploited to formulate the time adapted optimal control Lagrangian $\tilde{\mathcal{L}}$ based on $\tilde{\mathcal{H}}$. Euler-Lagrange equations derived from $\mathcal{L}$ provide necessary optimality conditions, assuming sufficient smoothness of the solution. Considering the time adapted optimal control Lagrangian, $\tilde{\mathcal{L}}$, new Euler-Lagrange equations can be derived that provide a set of necessary optimality conditions for the time adapted system.

3.4.1 Transformation from Optimal Control Hamiltonian to Lagrangian

Recalling that $L = \frac{\partial H}{\partial p} \cdot p - H$, the optimal control Lagrangian may be written

$$\mathcal{L} = \frac{\partial \mathcal{H}}{\partial p_{o.c.}} \cdot p_{o.c.} - \mathcal{H}, \tag{3.55}$$

where $p_{o.c.}$ is the momentum of the optimal control problem. Ordinarily, the momentum for a Hamiltonian system may be computed according to the equation

$$p = \frac{\partial L}{\partial \dot{q}}, \tag{3.56}$$

where q represents the state. For the optimal control problem, the state is augmented with the adjoint variable μ; therefore, denote the state and its derivative by

$$x = (q, \mu), \tag{3.57a}$$

$$\dot{x} = (\dot{q}, \dot{\mu}). \tag{3.57b}$$

Thus, the optimal control momentum is given by

$$p_{o.c.} = \frac{\partial \mathcal{L}}{\partial \dot{x}} = \left(\frac{\partial \mathcal{L}}{\partial \dot{q}}, \frac{\partial \mathcal{L}}{\partial \dot{\mu}} \right). \tag{3.58}$$

Consider the optimal control Lagrangian for the simple example in §3.3,

$$\mathcal{L} = \left(-\frac{1}{2}\mu^2 + \nu(\dot{q} - \dot{q}) + \mu\ddot{q} \right), \tag{3.59}$$

where ν and μ are the adjoint variables. Since variations of the action of the optimal control Lagrangian are important, consider the action of the optimal control Lagrangian,

$$\mathfrak{G}(q) = \int_0^T \left(-\frac{1}{2}\mu^2 + \nu(\dot{q} - \dot{q}) + \mu\ddot{q} \right) \, dt. \tag{3.60}$$

Integrating the term containing $\ddot{q}$ by parts and neglecting the boundary term (it will disappear when considering variations), the optimal control Lagrangian may be written,

$$\mathcal{L} = -\frac{1}{2}\mu^2 - \dot{\mu}\dot{q}. \tag{3.61}$$

Application of equation (3.58) gives the momentum

$$p_{o.c.} = \left(-\dot{\mu}, -\dot{q}\right), \tag{3.62}$$

and when applied in equation (3.55) generates the expression

$$\mathcal{L} = -\frac{\partial \mathcal{H}}{\partial(-\dot{q})}\dot{q} - \frac{\partial \mathcal{H}}{\partial(-\dot{\mu})}\dot{\mu} - \mathcal{H}, \tag{3.63}$$

where

$$\mathcal{H} = \frac{1}{2}\mu^2 + \nu\dot{q}. \tag{3.64}$$

Examination of the differential equations for the adjoint variables reveals that $\nu = -\dot{\mu}$ for this system, giving

$$\mathcal{H} = \frac{1}{2}\mu^2 - \dot{\mu}\dot{q}. \tag{3.65}$$

Application of equation (3.63) returns the expected expression for $\mathcal{L}$ given in equation (3.61).

For a more general optimal control problem with dynamics given by

$$\ddot{q} = F(q, \dot{q}) + G(q)u,$$

the optimal control Hamiltonian is given by

$$\mathcal{H} = -\frac{1}{2}u^2 + \nu\dot{q} + \mu\left(F(q,\dot{q}) + G(q)u\right). \tag{3.66}$$

Variations of this Hamiltonian with respect to u gives the expression for the optimal control

$$u = \mu G(q). \tag{3.67}$$

Therefore, the optimal control Lagrangian can be written

$$\mathcal{L} = -\frac{1}{2}G(q)^2\mu^2 - \mu F(q,\dot{q}) - \dot{\mu}\dot{q}. \tag{3.68}$$

It is assumed that $\frac{\partial^2 F}{\partial \dot{q}^2} = 0$. This assumption is valid for all problems discussed in this thesis. Based on this more general optimal control Lagrangian, the optimal control momentum is

$$p_{o.c.} = \left(-\dot{\mu} - \mu\frac{\partial F}{\partial \dot{q}}, -\dot{q}\right). \tag{3.69}$$

Note that for a mechanical system, the Lagrangian depends on q and $\dot{q}$, and it is written $L(q,\dot{q})$. For the optimal control problem, the optimal control Lagrangian depends on q, μ, $\dot{q}$, and $\dot{\mu}$, written $\mathcal{L}(q,\mu,\dot{q},\dot{\mu})$.

3.4.2 Transformation of Time Adapted Optimal Control Hamiltonian and Lagrangian

Recall that the time adapted Hamiltonian is given by $\tilde{H} = \sigma(q)(H - H_0)$. Therefore, the time adapted optimal control Hamiltonian is

$$\tilde{\mathcal{H}} = \sigma(q)\left(\mathcal{H} - \mathcal{H}_0\right), \tag{3.70}$$

where $\mathcal{H}_0$ replaces H_0 and is used to denote the initial value of the optimal control Hamiltonian, representing an energy of the optimal control problem. Consequently, the time adapted optimal control Lagrangian can be written

$$\tilde{\mathcal{L}} = \frac{\partial \tilde{\mathcal{H}}}{\partial p_{o.c.}} \cdot p_{c.o} - \tilde{\mathcal{H}} = \sigma(q) \left(\frac{\partial \mathcal{H}}{\partial p_{o.c.}} \cdot p_{c.o} - \mathcal{H} + \mathcal{H}_0 \right) = \sigma(q) \left(\mathcal{L} + \mathcal{H}_0 \right), \quad (3.71)$$

where the simplification on the right-hand side is possible under the assumption that $\sigma(q)$ is not a function of the optimal control problem momentum, $p_{o.c.}$. Using the same representation as for equation (3.10),

$$\tilde{\mathcal{L}}(\tau) = c_t'(\mathcal{L} + \mathcal{H}_0) + c_\lambda(c_t' - \sigma(c_q)). \quad (3.72)$$

The variation of the action is

$$\delta \tilde{\mathcal{L}}(\tau) = \delta \int_0^{\tau_f} \left[c_t'(\mathcal{L}(\tau) + \mathcal{H}_0) + c_\lambda(c_t' - \sigma(c_q)) \right] d\tau = 0, \quad (3.73)$$

with variations vanishing on the endpoints.

3.4.3 Time Adapted DMOC: Discrete Time Adapted Euler Lagrange Equations

The discrete time adapted action for the optimal control problem is given by

$$\widehat{S}_0^N = \sum_{k=0}^{N-1} \left[\mathcal{L}_d(q_k, q_{k+1}, \mu_k, \mu_{k+1}, h_k) + h_k \mathcal{H}_0 + \lambda_k(h_k - h\sigma(q_k, q_{k+1})) \right] \quad (3.74)$$

where

$$\begin{aligned} \mathcal{L}_d(q_k, q_{k+1}, \mu_k, \mu_{k+1}, h_k) = h_k \Bigg[& -\frac{1}{2} G \left(\frac{q_k + q_{k+1}}{2} \right)^2 \left(\frac{\mu_k + \mu_{k+1}}{2} \right)^2 \\ & - \left(\frac{\mu_k + \mu_{k+1}}{2} \right) F \left(\frac{q_k + q_{k+1}}{2}, \frac{q_{k+1} - q_k}{h_k} \right) - \left(\frac{\mu_{k+1} - \mu_k}{h_k} \right) \left(\frac{q_{k+1} - q_k}{h_k} \right) \Bigg], \end{aligned} \quad (3.75)$$

and $h_k = t_{k+1} - t_k$ and $h = \tau_{k+1} - \tau_k$ is a constant. Then, variations of the discrete action for the optimal control problem with respect to q_k, μ_k, t_k, and λ_k,

$$\delta \sum_{k=0}^{N-1} \left[\mathcal{L}_d(q_k, q_{k+1}, \mu_k, \mu_{k+1}, h_k) + h_k \mathcal{H}_0 + \lambda_k(h_k - h\sigma(q_k, q_{k+1})) \right] = 0, \quad (3.76)$$

generate the discrete time adapted Euler-Lagrange equations for the optimal control problem

$$\frac{\partial}{\partial q_k}\mathcal{L}_{k-1,k} + \frac{\partial}{\partial q_k}\mathcal{L}_{k,k+1} - h\lambda_k\frac{\partial\sigma(q_k,q_{k+1})}{\partial q_k} - h\lambda_{k-1}\frac{\partial\sigma(q_{k-1},q_k)}{\partial q_k} = 0, \tag{3.77a}$$

$$\frac{\partial}{\partial \mu_k}\mathcal{L}_{k-1,k} + \frac{\partial}{\partial \mu_k}\mathcal{L}_{k,k+1} = 0, \tag{3.77b}$$

$$\lambda_{k-1} - \lambda_k + \frac{\partial}{\partial t_k}\mathcal{L}_{k-1,k} - \frac{\partial}{\partial t_k}\mathcal{L}_{k,k+1} = 0, \tag{3.77c}$$

$$t_{k+1} - t_k - h\sigma(q_k,q_{k+1}) = 0, \tag{3.77d}$$

where $\mathcal{L}_{k-1,k} = \mathcal{L}_d(q_{k-1},q_k,\mu_{k-1},\mu_k,h_{k-1})$ and $\mathcal{L}_{k,k+1} = \mathcal{L}_d(q_k,q_{k+1},\mu_k,\mu_{k+1},h_k)$. Note that all variations of $\mathcal{H}_0$ vanish since it is a constant.

Equation (3.77a) are constraints equations for the adjoint variables, equation (3.77b) are equivalent to the usual discrete Euler-Lagrange equations, equation (3.77c) enforces preservation of the optimal control Hamiltonian function, and equation (3.77d) enforces the time adaption. Equations (3.77) serve as constraints that enforce the dynamics. Since the cost function is built into the Lagrangian, it is not necessary to enforce the cost function separately.

Boundary Conditions

The boundary conditions for configuration variable q are the same as for regular DMOC. That is, $q(0) = q_0$ and $q(T) = q_N$, as before. The momentum boundary conditions require more care. Recall that for the optimal control problem, there is an augmented state consisting of (q,μ). Consequently, there are discrete momentum variables p_q and p_μ computed according to the discrete Legendre transform,

$$p_{q_0} = -\frac{\partial}{\partial q_0}\mathcal{L}_d(q_0,q_1,\mu_0,\mu_1,h_0) + h\lambda_0\frac{\partial\sigma(q_0,q_1)}{\partial q_0}, \tag{3.78a}$$

$$p_{\mu_0} = -\frac{\partial}{\partial \mu_0}\mathcal{L}_d(q_0,q_1,\mu_0,\mu_1,h_0), \tag{3.78b}$$

$$p_{q_N} = \frac{\partial}{\partial q_N}\mathcal{L}_d(q_{N-1},q_N,\mu_{N-1},\mu_N,h_{N-1}) - h\lambda_N\frac{\partial\sigma(q_{N-1},q_N)}{\partial q_N}, \tag{3.78c}$$

$$p_{\mu_N} = \frac{\partial}{\partial \mu_N}\mathcal{L}_d(q_{N-1},q_N,\mu_{N-1},\mu_N,h_{N-1}). \tag{3.78d}$$

The continuous momentum boundary values are determined via the continuous Legendre transform, and the boundary conditions are given by

$$\frac{\partial \mathcal{L}(q_0, \dot{q}_0)}{\partial \dot{q}_0} - p_{q_0} = 0, \tag{3.79a}$$

$$\frac{\partial \mathcal{L}(q_0, \dot{q}_0)}{\partial \dot{\mu}_0} - p_{\mu_0} = 0, \tag{3.79b}$$

$$\frac{\partial \mathcal{L}(q_N, \dot{q}_N)}{\partial \dot{q}_N} - p_{q_N} = 0, \tag{3.79c}$$

$$\frac{\partial \mathcal{L}(q_N, \dot{q}_N)}{\partial \dot{\mu}_N} - p_{\mu_N} = 0. \tag{3.79d}$$

External Forces

This formulation is valid even for systems with external forces in addition to control forces. The external forces are included in $F(q, \dot{q})$ as part of the dynamics. If the system is subject to a time-dependent external force, the dynamics are given by

$$\ddot{q} = F(q, \dot{q}) + G(q)u + F_t(q, t),$$

where $F_t(q, t)$ represents the time-dependent external force. Then, the optimal control Lagrangian is

$$\mathcal{L} = -\frac{1}{2}G(q)^2\mu^2 - \mu F(q, \dot{q}) - \dot{\mu}\dot{q} - \mu F_t(q, t). \tag{3.81}$$

The discrete version of this forced optimal control Lagrangian replaces $\mathcal{L}_d$ in equation (3.74), and variations of this new time adapted Lagrangian should be zero, leading to new Euler-Lagrange equations including both control forces and external forces. Furthermore, the momentum boundary conditions are still given by equations (3.79).

3.4.4 Time Adaptive DMOC: an Indirect Method

Even though DMOC is a direct method for optimal control, formulation of time adapted DMOC as described in §3.4.3 actually results in an indirect method for solving the optimal control problem. Equations (3.77) combined with the boundary conditions describe a boundary value problem, which can be solved with any BVP solver. For the solution of all examples in this chapter, the implementation is nearly identical to regular DMOC with the Euler-Lagrange equations and boundary conditions enforced as constraints and with cost function set to one. Then the SQP solver SNOPT determines the feasible solution, which in this case is the locally optimal solution.

Table 3.1 demonstrates the parallels between the Lagrangian of the mechanical system, L, and the optimal control Lagrangian, $\mathcal{L}$, for continuous and discrete settings. Variations of the action of the Lagrangian of the mechanical system lead to the Euler-Lagrange (EL) equations of motion. Variations of the action of the time adapted Lagrangian, $\tilde{L}$, lead to the time adapted (TA) Euler-Lagrange equations of motion. Variations of the action of the optimal control Lagrangian lead to necessary optimality conditions (nec. opt. cond.), and time adapted necessary optimality conditions (TA nec. opt. cond.) result for the time adapted optimal control Lagrangian. The discrete versions are denoted by D.

Table 3.1: TIme Adaption Comparison

Continuous		Discrete	
L	$\tilde{L}$	L_d	$\tilde{L}_d$
$\Downarrow$	$\Downarrow$	$\Downarrow$	$\Downarrow$
EL equations	TA EL equations	DEL equations	TA DEL equations
$\mathcal{L}$	$\tilde{\mathcal{L}}$	$\mathcal{L}_d$	$\tilde{\mathcal{L}}_d$
$\Downarrow$	$\Downarrow$	$\Downarrow$	$\Downarrow$
nec. opt. cond.	TA nec. opt. cond.	D nec. opt. cond.	DTA nec. opt. cond.

3.4.5 Results for Simple Example

Consider again the simple example with $L = \frac{1}{2}\dot{q}^2$, dynamics $\ddot{q} = u$, and time adapted according to $\sigma = \frac{q}{2}$. Taking variations of $\mathcal{H}$ with respect to u gives that

$u = \mu$, and the optimal control Lagrangian is

$$\mathcal{L} = -\frac{1}{2}\mu^2 - \dot{\mu}\dot{q}. \tag{3.82}$$

The discrete action principle is

$$\delta \sum_{k=0}^{N-1} \Bigg[-\frac{h_k}{2}\left(\frac{\mu_k + \mu_{k+1}}{2}\right)^2 - h_k \left(\frac{\mu_{k+1} - \mu_k}{h_k}\right)\left(\frac{q_{k+1} - q_k}{h_k}\right) + h_k \mathcal{H}_0 \\ + \lambda_k \left(h_k - h\left(\frac{q_k + q_{k+1}}{4}\right)\right)\Bigg] = 0. \tag{3.83}$$

Variations of the discrete action principle with respect to q_k, μ_k, t_k, and λ_k generate the discrete time adapted Euler-Lagrange equations for the optimal control problem,

$$\left(\frac{\mu_{k+1} - \mu_k}{h_k}\right) - \left(\frac{\mu_k - \mu_{k-1}}{h_{k-1}}\right) - \frac{h}{4}\lambda_k - \frac{h}{4}\lambda_{k-1} = 0, \tag{3.84a}$$

$$\left(\frac{q_{k+1} - q_k}{h_k}\right) - \left(\frac{q_k - q_{k-1}}{h_{k-1}}\right) - \frac{h_k}{2}\left(\frac{\mu_k + \mu_{k+1}}{2}\right) \\ -\frac{h_{k-1}}{2}\left(\frac{\mu_{k-1} + \mu_k}{2}\right) = 0, \tag{3.84b}$$

$$\lambda_{k-1} - \lambda_k + \left(\frac{q_k - q_{k-1}}{h_{k-1}}\right)\left(\frac{\mu_k - \mu_{k-1}}{h_{k-1}}\right) - \frac{1}{2}\left(\frac{\mu_{k-1} + \mu_k}{2}\right) \\ - \left(\frac{q_{k+1} - q_k}{h_k}\right)\left(\frac{\mu_{k+1} - \mu_k}{h_k}\right) + \frac{1}{2}\left(\frac{\mu_k + \mu_{k+1}}{2}\right) = 0, \tag{3.84c}$$

$$t_{k+1} - t_k - h\left(\frac{q_k + q_{k+1}}{4}\right) = 0. \tag{3.84d}$$

Recall that the momentum for this example is $p_{o.c.} = (-\dot{\mu}, -\dot{q})$. Therefore, the momentum boundary conditions given in equation (3.79) can be written as

$$-\dot{\mu}_0 - p_{q_0} = 0, \qquad -\dot{q}_0 - p_{\mu_0} = 0,$$
$$-\dot{\mu}_N - p_{q_N} = 0, \qquad -\dot{q}_N - p_{\mu_N} = 0.$$

For this example, the initial and final discrete configurations must equal the continuous ones:

$$q(0) = q_0, \tag{3.85a}$$

$$q(T) = q_N. \tag{3.85b}$$

Next, the initial and final velocity values should be enforced; consequently, the boundary conditions including $\dot{q}_0$ and $\dot{q}_N$ should also be enforced,

$$-\dot{q}_0 - p_{\mu_0} = 0, \tag{3.86a}$$

$$-\dot{q}_N - p_{\mu_N} = 0. \tag{3.86b}$$

Furthermore, initial conditions for time and λ are included such that $t_0 = 0$ and $\lambda_0 = 0$. These boundary conditions are sufficient for a well-posed boundary value problem, so the boundary conditions for p_q need not be enforced.

Examining equation (3.86a), and since $\lambda_0 = 0$ by definition, this constraint simplifies to

$$-\dot{q}_0 + \left(\frac{q_1 - q_0}{h_0}\right) + \frac{h_0}{2}\left(\frac{\mu_0 + \mu_1}{2}\right) = 0, \tag{3.87}$$

which looks very similar to the usual momentum boundary condition with $\left(\frac{\mu_0+\mu_1}{2}\right) = u_0$.

Using the simple initial guess described in §3.3, this time adapted form of DMOC successfully produces the correct optimal solution. If the final time is held fixed with time adapted DMOC, the problem is over-constrained. Allowing the final time to vary, time adapted DMOC finds an optimal solution with a slightly different final time than the initial guess. A different final time means that the boundary conditions are slightly different, and therefore, so is the optimal solution. To verify that time adapted DMOC generates the correct optimal solution, the optimal solution is used as an initial guess for regular DMOC. In this way, the optimal solutions from regular DMOC and time adapted DMOC can be compared because they share the same time grid. Figure 3.3 compares the time adapted DMOC optimal solution with the regular DMOC optimal solution for both the optimal trajectory and optimal control. As shown in the figure, the solutions match, confirming that time adapted DMOC converges to the correct optimal solution.

Two different energy metrics are examined to compare the DMOC and time adapted DMOC solutions. First, the discrete energy drift,

$$E_d = E_{k+1} - E_1 - \sum_{i=1}^{k} f_{i-1}^{+}(q_j - q_{j-1}) + f_i^{-}(q_{j+1} - q_j), \tag{3.88}$$

for regular DMOC, and

$$E_d = E_{k+1} - E_1, \tag{3.89}$$

for time adapted DMOC, where

$$E_{k+1} = -D_3 L_d(q_k, q_{k+1}, t_{k+1} - t_k) \text{ for regular DMOC,}$$
$$E_{k+1} = -D_5 \mathcal{L}_d(q_k, q_{k+1}, \mu_k, \mu_{k+1}, t_{k+1} - t_k) \;\text{ for time adapted DMOC,}$$

should converge to zero with second-order convergence. Since the expressions for discrete energy drift are different for DMOC and time adapted DMOC, it is also useful to consider the discrete version of

$$\Delta E_c = E_c(t) - E_c(0), \tag{3.90}$$

where

$$E_c(t) = E(t) - \int_0^t f(q(s), \dot{q}(s), u(s))\dot{q}(s)\; ds, \tag{3.91}$$

and $E(t)$ represents the total energy at each time. The integral term represents the energy injected into the system by the control forces. The discrete Legendre transform is employed to compute the momenta and corresponding velocities at each node, which are then used to compute the discrete version of equation (3.90).

Figure 3.5 shows the convergence for errors in position and control for regular DMOC with constant step size, regular DMOC with time adapted initial guess (time adapted variational integrators generate an initial guess with variable time grid; this time grid is held fixed), and time adapted DMOC. Both plots display the expected second-order convergence. Notice that the errors are slightly smaller for regular DMOC with constant step size. This is not too surprising since the time adaption is arbitrary.

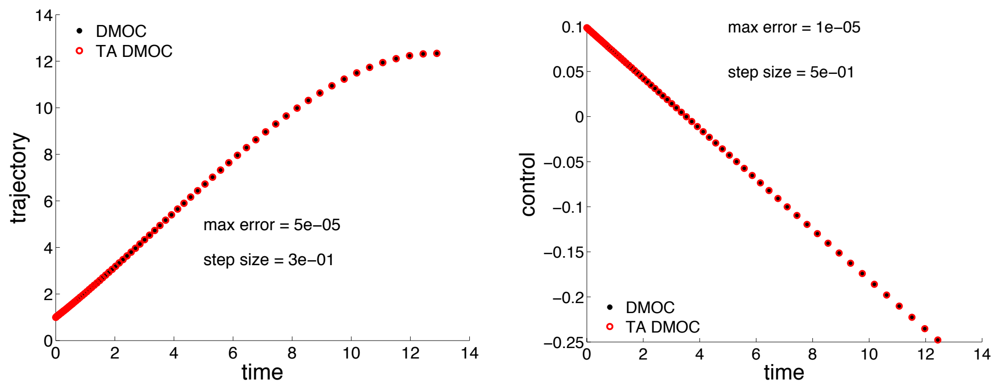

(a) Position, q (b) Control force, u

Figure 3.2: Simple example: regular DMOC and time adapted DMOC generate the same optimal (a) trajectory and (b) control

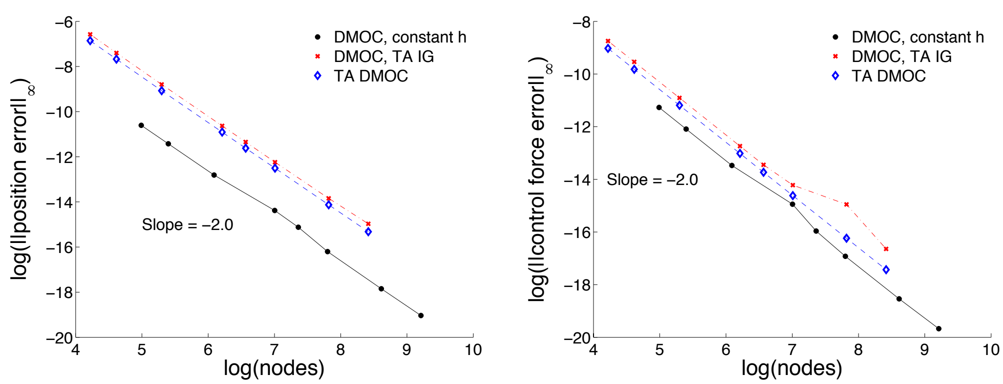

(a) Convergence for position error (b) Convergence for control force error

Figure 3.3: Simple example: comparison of solution error for regular DMOC with constant step size, regular DMOC with time adapted initial guess, and time adapted DMOC. The error in (a) position and (b) control force converges to zero with a slope of -2.

The energy metrics, E_d and ΔE_c, are compared for regular DMOC and time adapted DMOC in Figures 3.4(a) and (b), respectively. Note that the energy metric is better for time adapted DMOC in both instances. Figure 3.5(a) shows the rate of convergence for λ, which converges to zero with second-order convergence as predicted. Figure 3.5(b) displays the log of minimum step size versus the log of CPU time in seconds. For most minimum step sizes, time adapted DMOC converges faster than regular DMOC with constant step size and regular DMOC with time adapted initial guess. Also, it should be noted that as the minimum step size decreases, regular DMOC with time adapted initial guess starts having convergence problems. In comparison, time adapted DMOC converges to the optimal solution every time with stringent tolerances. It is interesting to note that time adapted DMOC includes optimization variables q_k, μ_k, t_k, and λ_k compared to just q_k and u_k for regular DMOC. Even with twice as many optimization variables, time adapted DMOC still converges faster.

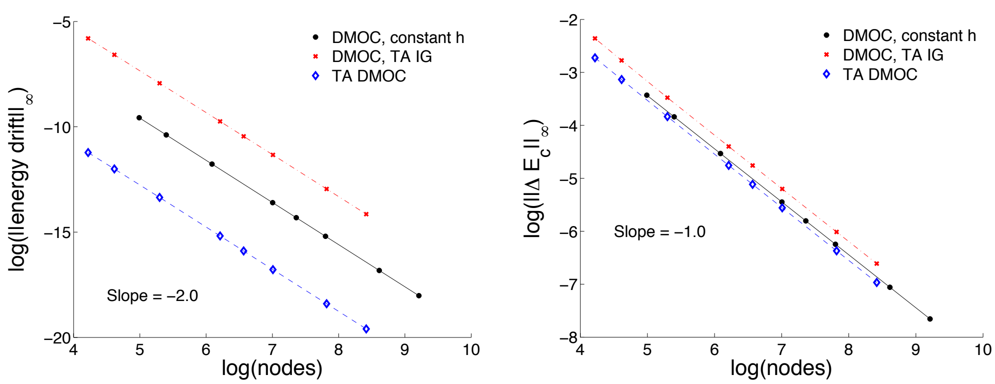

(a) Convergence of E_d (b) Convergence of ΔE_c

Figure 3.4: Simple example: comparison of energy behavior with regular DMOC with constant step size or time adapted initial guess and time adapted DMOC. Convergence of (a) discrete energy drift, E_d, and (b) ΔE_c.

3.5 Examples

Several different examples are presented that demonstrate different aspects of DMOC with time adaption. First, the elliptical orbit transfer problem is solved using time adaptive DMOC. For this problem, the control force is defined by $f = ru$,

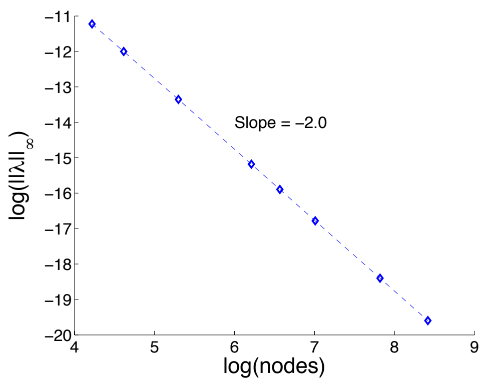

(a) Convergence of λ

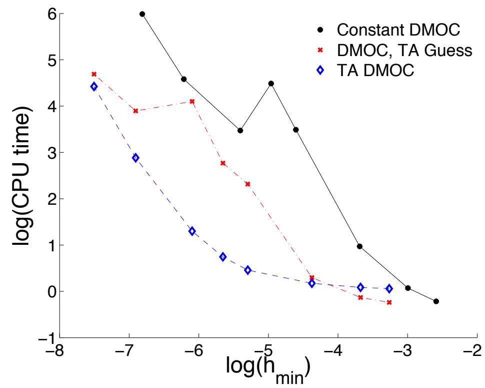

(b) Computation time

Figure 3.5: Simple example: convergence of (a) λ, and (b) log-log plot of minimum step size versus CPU time in seconds. In most cases, time Adapted DMOC converges fastest.

where r is a configuration variable. Therefore, in contrast to the simple example, $g(q) \neq 1$. Also, $f(q, \dot{q})$ is nonzero. Next, the problem of reconfiguring a cubesat is presented, demonstrating another potential application for time adapted DMOC.

3.5.1 Elliptical Orbit Transfer

The elliptical orbit transfer is presented in 2d-polar coordinates, $q = (r, \varphi)$. From before, a spacecraft orbits a body in an elliptical orbit such that after one full orbit, it enters a slightly different orbit with a larger apogee radius. The Lagrangian for this system is

$$L(q, \dot{q}) = \frac{1}{2} m(\dot{r}^2 + r^2 \dot{\varphi}^2) + \frac{GMm}{r}, \tag{3.92}$$

where G is the universal constant of gravitation, M is the mass of the primary body, and m is the mass of the satellite. To best illustrate the effects of time adaption, the problem is scaled such that $m = 1$ and $GM = 1$. Configuration variables r and φ represent the radial distance of the spacecraft from the center of the primary body and the angular position of the spacecraft with respect to the line through the primary body and the perigee of the elliptical orbit, respectively.

The controlled dynamics of the system are

$$\ddot{r} = r\dot{\varphi}^2 - \frac{GM}{r^2}, \tag{3.93a}$$

$$\ddot{\varphi} = -2\frac{\dot{r}}{r}\dot{\varphi} + \frac{u}{rm}. \tag{3.93b}$$

Aiming to minimize the control effort, the optimal control Hamiltonian is

$$\mathcal{H} = -\frac{1}{2}u^2 + \nu_r\dot{r} + \nu_\varphi\dot{\varphi} + \mu_r\left(r\dot{\varphi}^2 - \frac{GM}{r^2}\right) + \mu_{\varphi},\left(-2\frac{\dot{r}}{r}\dot{\varphi} + \frac{u}{rm}\right), \tag{3.94}$$

and $\frac{\partial\mathcal{H}}{\partial u} = 0$ requires that $u = \frac{\mu_\varphi}{rm}$. Thus, the optimal control Lagrangian is

$$\mathcal{L} = -\frac{1}{2}\left(\frac{\mu_\varphi}{rm}\right)^2 - \mu_r\left(r\dot{\varphi}^2 - \frac{GM}{r^2}\right) + \mu_\varphi\left(2\frac{\dot{r}}{r}\dot{\varphi}\right) - \dot{\mu}_r\dot{r} - \dot{\mu}_\varphi\dot{\varphi}. \tag{3.95}$$

Using the discrete version of this Lagrangian in equation (3.76) generates the discrete Euler-Lagrange equations to be enforced as constraints. The spacecraft begins in an elliptical orbit with $r_{p1} = 1$ and $r_{a1} = 2$. The spacecraft ends in an elliptical orbit with the same perigee and $r_{a2} = 4$. The boundary conditions to be enforced include $r_0 = 1$, $r_N = 4$, $\varphi_0 = 0$, $\varphi_N = \pi$, $\dot{r}_0 = \dot{r}_N = 0$, $\dot{\varphi}_0 = \frac{1}{r_{p1}}\sqrt{GM(\frac{2}{r_{p1}} - \frac{1}{a_1})}$, and $\dot{\varphi}_N = \frac{1}{r_{a_2}}\sqrt{GM(\frac{2}{r_{a_2}} - \frac{1}{a_2})}$, where $a = \frac{1}{2}(r_p + r_a)$ is the semi-major axis of the ellipse.

Several time adaption strategies are tested, given by

$$\sigma_1 = \frac{1}{\sqrt{E_0 - W\left(\frac{q_k+q_{k+1}}{2}\right) + \nu}}, \tag{3.96}$$

$$\sigma_2 = \frac{1}{\sqrt{E_0 - W\left(\frac{q+k+q_{k+1}}{2}\right) + \left|\left|\nabla W\left(\frac{q+k+q_{k+1}}{2}\right)\right|\right|^2 + \nu}}, \tag{3.97}$$

$$\sigma_3 = \frac{1}{\left|\left|\nabla W(q_k) + \nabla W(q_{k+1}) + \nu\right|\right|}, \tag{3.98}$$

where $W = \frac{GM}{r}$ is the potential energy, E_0 is the initial energy, $||\cdot||$ denotes the 2-norm, and ν is a small constant.

Figure 3.6 compares the optimal trajectories for time adapted DMOC and regular DMOC using the time adapted solution as initial guess. Figure 3.7 compares the optimal control solutions. As shown in the both figures, the optimal solutions from time adapted DMOC and regular DMOC match for all three time adaption strategies.

Figure 3.8 compares the energy metrics, E_d and ΔE_c. As shown in Figure 3.8(a), the discrete energy drift for solutions generated with time adapted DMOC is smaller than the discrete energy drift for regular DMOC, even with time adapted initial guess. For ΔE_c, shown in Figure 3.8(b), time adapted DMOC produces slightly better results than regular DMOC.

Figure 3.9(a) displays the convergence of λ for all three time adaption strategies. As expected, λ approaches zero with second order convergence. Figure 3.9(b) exhibits the log of minimum step size versus log of the computation time. Time adapted DMOC converges faster than regular DMOC with constant step size or time adapted initial guess. As the minimum step size decreases, convergence with regular DMOC becomes less dependable, but time adapted DMOC continues to converge very well. Since an analytical solution to this optimal control problem does not exist, convergence plots of the error in configuration or control are not included.

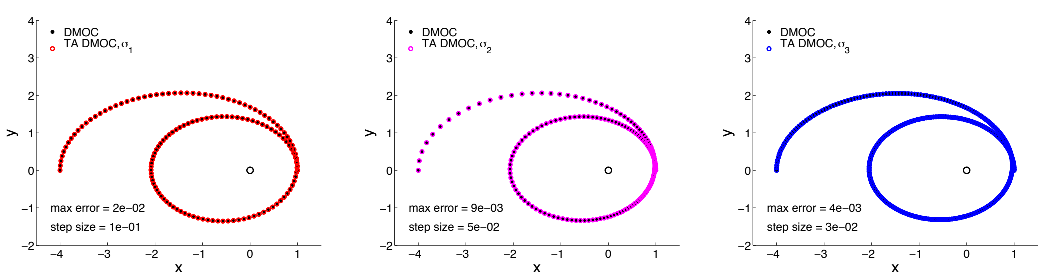

(a) σ_1 (b) σ_2 (c) σ_3

Figure 3.6: Elliptical orbit transfer: optimal trajectory for regular DMOC and time adapted DMOC with (a) σ_1, (b) σ_2, and (c) σ_3. The same optimal solution is achieved using DMOC and time adapted DMOC.

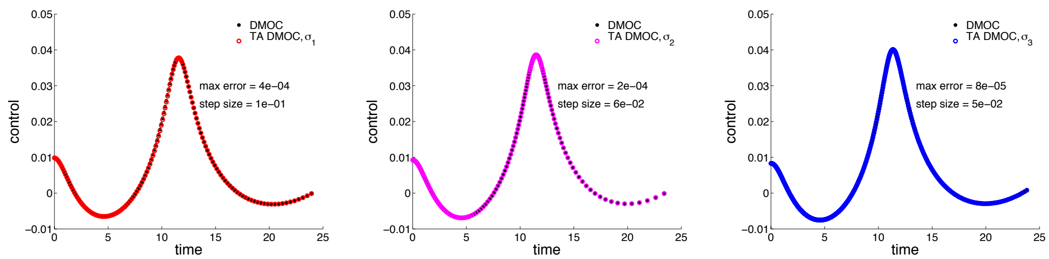

(a) σ_1 (b) σ_2 (c) σ_3

Figure 3.7: Elliptical orbit transfer: optimal control for regular DMOC and time adapted DMOC with (a) σ_1, (b) σ_2, and (c) σ_3. The same optimal solution is achieved using DMOC and time adapted DMOC.

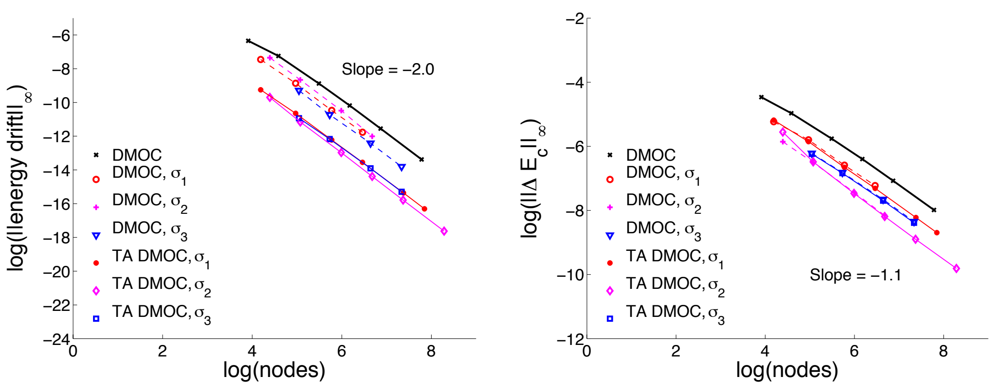

(a) Convergence of E_d (b) Convergence of ΔE_c

Figure 3.8: Elliptical orbit transfer: comparison of energy behavior. Convergence of (a) discrete energy drift, E_d, and (b) ΔE_c.

3.5.2 Cubesat Reconfiguration

This example is modeled on the hovercraft reconfiguration example presented by [6] and is applicable to the KISS reconfigurable modular telescope project. Consider a cubesat with configuration described by position, (x, y), and orientation, θ. The cubesat is to be moved from some initial configuration (x_0, y_0, θ_0) to a final configuration (x_N, y_N, θ_N) using optimal control. It is controlled by two control forces, f_1 and f_2, applied at a distance r from the center of mass such that f_1 acts in the direction of motion, and f_2 acts perpendicular to the motion. The

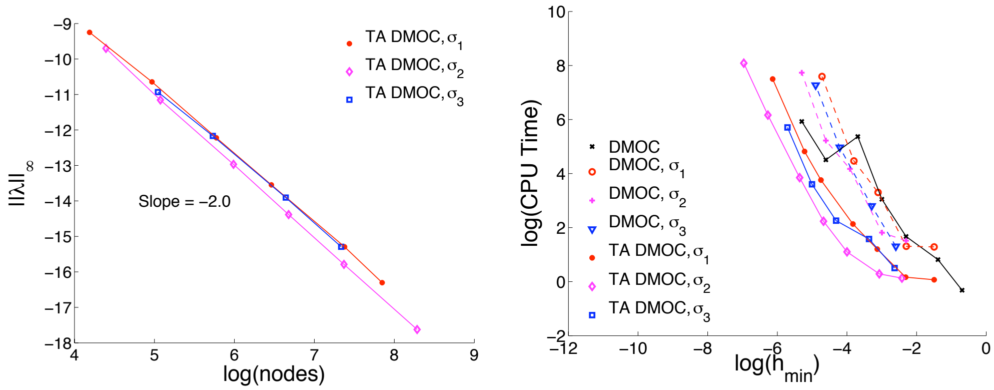

(a) Convergence of λ (b) Computation time

Figure 3.9: Elliptical orbit transfer: convergence of (a) λ. (b) Log of computation time versus log of minimum step size shows that the time adapted solutions converge fastest.

Lagrangian of this system describes the kinetic energy of the cubesat,

$$L(q, \dot{q}) = \frac{1}{2}(m\dot{x}^2 + m\dot{y}^2 + J\dot{\theta}^2), \tag{3.99}$$

where m is the mass and J is the moment of inertia. For this example, m and J both equal one. The controlled equations of motion are given by

$$\ddot{x} = f_1 \cos(\theta) - f_2 \sin(\theta) \tag{3.100a}$$

$$\ddot{y} = f_1 \sin(\theta) + f_2 \cos(\theta) \tag{3.100b}$$

$$\ddot{\theta} = -r f_2. \tag{3.100c}$$

Aiming to minimize control effort, the optimal control Lagrangian, in terms of the state and adjoint variables, is

$$\mathcal{L} = -\frac{1}{2}\left(\mu_x^2 + \mu_y^2 + r^2\mu_\theta^2 + 2r\mu_\theta\left(\mu_x \sin(\theta) - \mu_y \cos(\theta)\right)\right) - \dot{\mu}_x\dot{x} - \dot{\mu}_y\dot{y} - \dot{\mu}_\theta\dot{\theta}. \tag{3.101}$$

Time is adapted according to

$$\sigma = x^2 + y^2, \tag{3.102}$$

generating smaller time steps when the cubesat moves closer to its target location, located near the origin. The square of the distance from the origin is used for simplicity when deriving the constraint equations.

An initial guess is optimized first using time adapted DMOC. This optimal solution is then used as an initial guess for regular DMOC to verify that both methods converge to the same optimal solution. Figure 3.10 demonstrates that regular DMOC and time adapted DMOC generate the same optimal solution.

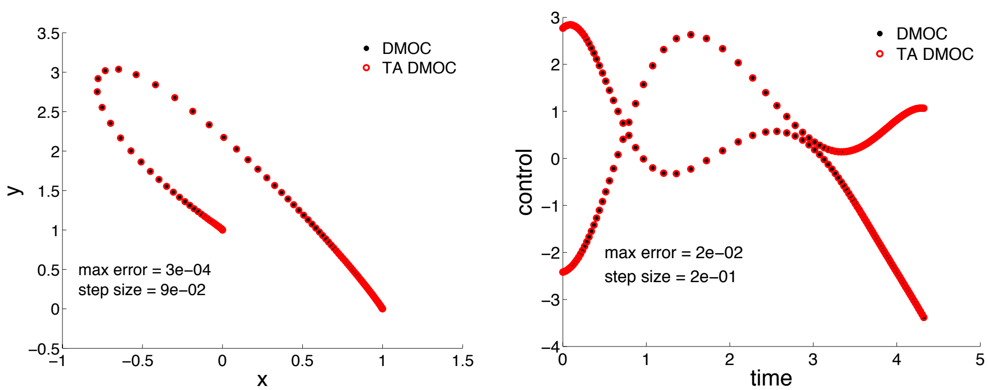

(a) Optimal trajectory (b) Optimal control

Figure 3.10: Cubesat reconfiguration: regular DMOC and time adapted DMOC generate the same optimal solution for the (a) trajectory and (b) control forces f_1 and f_2.

Figure 3.11 compares the energy metrics, E_d and ΔE_c. As shown in the plots, time adapted DMOC produces smaller values for both the discrete energy drift and ΔE_c. Figure 3.12(a) shows that λ converges to zero with second order convergence as expected. Figure 3.12(b) compares the computation time, and in contrast to the other examples, time adapted DMOC is slower than regular DMOC for this example because σ is not a function of the dynamics.

3.6 Conclusion

The process used to derive time adapted variational integrators can be applied to the optimal control problem, leading to a time adaptive form of DMOC. Time adapted DMOC is now an indirect approach to solving the optimal control problem

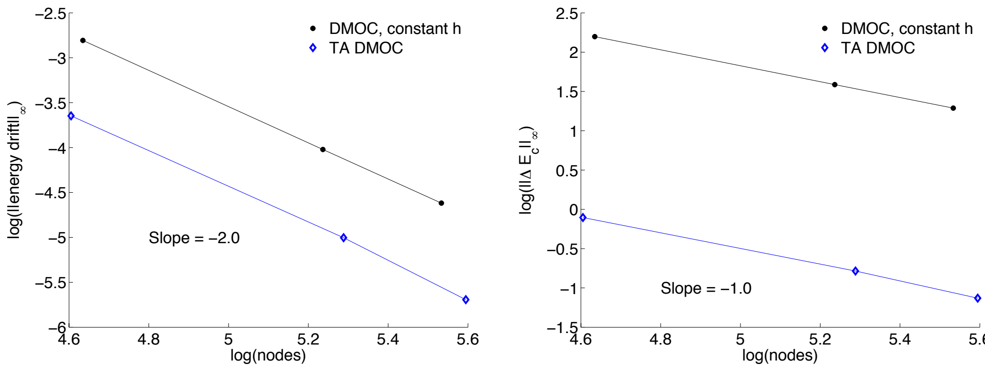

(a) Convergence of E_d (b) Convergence of ΔE_c

Figure 3.11: Cubesat reconfiguration: energy comparison. (a) Discrete energy, E_d, converges to zero with a slope of -2, as expected. (b) ΔE_c is smaller for time adapted DMOC. Time adapted DMOC produces solutions with smaller errors for both energy metrics.

even though regular DMOC is a direct optimization method. Variations of the discrete action of the time adapted optimal control Lagrangian with respect to the state, time, and adjoint variables lead to discrete Euler-Lagrange equations that serve as constraints. The problem is now a boundary value problem, and it is sufficient to set the cost function equal to one. The problem may be solved using SQP as before, but it may also be solved using another BVP solver.

The method is first tested on a very simple example with an analytical optimal control solution to verify that the method produces correct optimal control solutions. Then, it is tested on more relevant examples including the elliptical orbit transfer and the reconfiguration of a cubesat. It should be noted that since time is an optimization variable that changes throughout the optimization, the optimal solutions are slightly different than those achieved with regular DMOC. This is due to the difference in final time. The time adapted optimal solutions are verified by using them as initial guesses for regular DMOC, which then produces the same optimal solution.

While it is desirable to enforce a constraint on the final time, it appears that such a constraint over-constrains the problem. While a variable final time is fine for many problems, some problems may require a fixed final time, so this issue

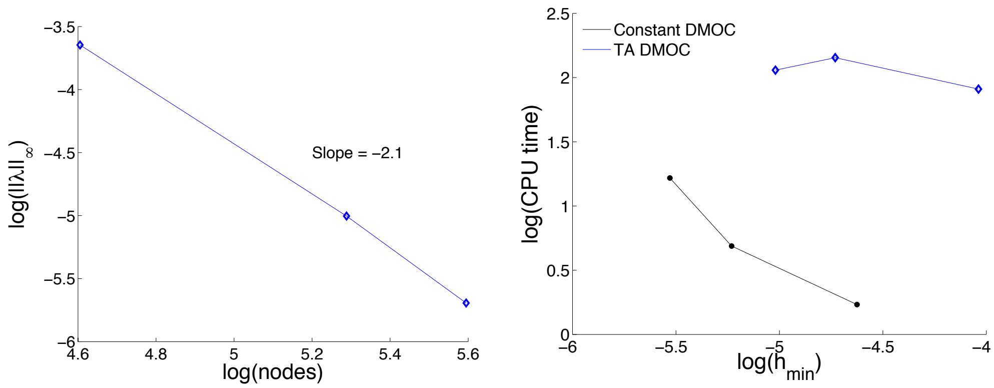

(a) Convergence of λ (b) Computation time

Figure 3.12: Cubesat reconfiguration: convergence of (a) λ, and (b) log of computation time versus log of minimum step size shows that the time adapted solutions general converge slower than regular DMOC because σ is not a function of the dynamics.

warrants further exploration. It is notable that while regular DMOC consists of optimization variables q and u, and time adapted DMOC has twice as many optimization variables, q, μ, t, and λ, time adapted DMOC converges faster than regular DMOC in most cases for which σ is a function of the dynamics. Also, as shown in the examples, time adapted DMOC displays the same energy convergence rate as regular DMOC, verifying that the energy drift is bounded for time adapted DMOC, just as it is for regular DMOC. Furthermore, as predicted λ converges to zero, verifying that the time adapted system converges to the regular system. Overall, time adapted DMOC provides a great optimization method for highly nonlinear problems for which variable step size is absolutely necessary.

Chapter 4

Conclusions and Future Work

This work demonstrates how the optimal control algorithm DMOC can be used for space mission problems and how to better adapt it for such nonlinear problems. The development of a fully time adapted version of DMOC is presented. Proper application of time adaption requires that Hamilton's principle be applied to the time adapted Lagrangian of the optimal control problem, instead of to the Lagrangian of the mechanical system. Therefore, instead of discretizing the Lagrange-d'Alembert principle, discretization of Hamilton's principle leads to discrete Euler-Lagrange equations that serve as constraints for a boundary value problem. This problem can be solved in the same way as regular DMOC using SQP, but with the cost function set to one. It should be noted that this formulation of time adapted DMOC is an indirect optimization method even though regular DMOC is a direct method. Optimization employing time adapted DMOC is demonstrated for the elliptical orbit transfer problem and the reconfiguration of a cubesat. Time adaptive DMOC proves to be efficient and accurate, preserving the energy and convergence properties of regular DMOC.

Time adaptive DMOC may potentially be used to design and optimize the reconfiguration maneuvers necessary for the KISS study on a reconfigurable modular space telescope. Each cubesat must be moved from the launch configuration to the operating configuration and the motion as the cubesat approaches docking is especially important. In particular, since the dynamics are potentially very nonlinear for docking, it is important to use very small step sizes, whereas large step sizes may be sufficient for large portions of the reconfiguration maneuver away from docking. For this reason, time adaptive DMOC may be more suitable for this problem than regular DMOC or another optimization method.

There are many possibilities for future work focusing on time adaptive DMOC. The version of time adapted DMOC proposed here requires that the final time be unconstrained. This could be undesirable for some problems, so a method that allows the final time to be fixed should be explored. In addition, since time adaption leads to an indirect optimization method, a different formulation for time adapted DMOC that preserves its status as a direct method should be examined. Also, it would be interesting to compare time adapted DMOC with regular DMOC using initial guesses employing Bett's mesh refinement strategy to design the time grid. Which strategy generates the most accurate optimal solutions? Furthermore, it is unclear whether time adaption is possible with $\sigma(q, t)$ instead of $\sigma(q)$. For example, the optimization of a trajectory from the Earth to the Moon, for which the potential forces from the Moon are time dependent, would require $\sigma(q, t)$ to ensure finer time stepping near the Moon. However, defining the time grid based on time is rather circular, so this problem should be handled with care.

Bibliography

[1] J. T. Betts. Survey of numerical methods for trajectory optimization. *AIAA J. Guidance, Control, and Dynamics*, 21(2):193–207, 1998.

[2] T. Binder, L. Blank, H. G. Bock, R. Bulirsch, W. Dahmen, M. Diehl, T. Kronseder, W. Marquardt, J. P. Schlöder, and O. von Stryk. Introduction to model based optimization of chemical processes on moving horizons. In M. Grötschel, S. O. Krumke, and J. Rambau, editors, *Online Optimization of Large Scale Systems: State of the Art*, pages 295–340. Springer, Berlin, 2001.

[3] R. C. Fetecau, J. E. Marsden, M. Ortiz, and M. West. Nonsmooth lagrangian mechanics and variational collision integrators. *SIAM Journal of Applied Dynamical Systems*, 2(3):381–416, 2003.

[4] P. E. Gill, W. Murray, and M. A. Saunders. SNOPT: An SQP algorithm for large-scale constrained optimization. *Report NA 97-2*, Department of Mathematics, University of California, San Diego, CA, USA, 1997.

[5] E. Hairer, C. Lubich, and G. Wanner. *Geometric Numerical Integration.* Springer-Verlag, Berlin, 2002.

[6] O. Junge, J. E. Marsden, and S. Ober-Blöbaum. Discrete mechanics and optimal control. In *Proceedings of the 16th IFAC World Congress*, 2005.

[7] L. Kharevych. *Geometric Interpretation of Physical Systems for Improved Elasticity Simulations.* Ph.D. thesis, California Institute of Technology, 2010.

[8] B. Leimkuhler and S. Reich. *Simulating Hamiltonian Dynamics*. Cambridge University Press, Cambridge, 2004.

[9] J. E. Marsden and M. West. Discrete mechanics and variational integrators. *Acta Numerica*, 10:357–514, 2001.

[10] A. Moore, S. Ober-Blöbaum, and J. E. Marsden. Mesh refinement strategies for spacecraft trajectory optimization using discrete mechanics and optimal control. In *AAS/AIAA Space Flight Mechanics Meeting, AAS 11-127*, 2011.

[11] S. Ober-Blöbaum. *Discrete Mechanics and Optimal Control*. Ph.D. thesis, University of Paderborn, 2008.

[12] S. Ober-Blöbaum, O. Junge, and J. E. Marsden. Discrete mechanics and optimal control: An analysis. *Control, Optimisation and Calculus of Variations*, 2010.

[13] L. S. Pontryagin, V. G. Boltyanski, R. V. Gamkrelidze, and E. F. Miscenko. *The Mechanical Theory of Optimal Processes*. John Wiley & Sons, 1962.